**Article ID:** 1007-4627(2015) 01-0001-023

# Importance of Triaxiality in Shape Transitions and Coexistence in $A \sim 100$ to 126 Neutron-rich Nuclei with $Z$ Beyond and Below Ru

Y. X. LUO (罗亦孝)[1, 2], J. H. Hamilton[1], J. O. Rasmussen[2, 3], A. V. Ramayya[1], S. Frauendorf[4, 5], E. WANG (王恩宏)[1], J. K. Hwang[1], J. G. WANG (王建国)[6], H. J. LI (李红洁)[6], E. Y. Yeoh (杨韵颐)[6], S.J. ZHU (朱胜江)[1, 6], Y. X. LIU (刘艳鑫)[7], C. F. JIAO (焦长峰)[8], W. Y. LIANG (梁午阳)[8], Yue SHI (石跃)[8], F. R. XU (许甫荣)[8], Y. SUN (孙扬)[9, 10], S. H. LIU (刘少华)[1, 11], N. T. Brewer[1, 12], I. Y. Lee[2], G. M. Ter-Akopian[13], A. V. Daniel[13], Yu. Oganessian[13], M. A. Stoyer[14], R. Donangelo[15], W. C. MA (马文超)[16]

(*1. Physics Department, Vanderbilt University, Nashville, TN 37235, USA;*
*2. Lawrence Berkeley National Laboratory, Berkeley, CA 94720, USA;*
*3. Department of Chemistry, U.C. Berkeley, Berkeley, CA 94720, USA;*
*4. Department of Physics, University of Notre Dame, Notre Dame IN 46556, USA;*
*5. Institut für Strahlenphysik, FZD-Rossendorf, Postfach, D-01314 Dresden, Germany;*
*6. Department of Physics, Tsinghua University, Beijing 100084, China;*
*7. School of Science, Huzhou Teachers College, Huzhou 31300, Zhejiang, China;*
*8. School of Physics, Peking University, Beijing 100871, China;*
*9. Department of Physics and Astronomy, Shanghai Jiao Tong University, Shanghai 200240, China;*
*10. Institute of Modern Physics, Chinese Academy of Sciences, Lanzhou 730000, China;*
*11. Chemistry Department, University of Kentucky, Lexington, KY 40505, USA;*
*12. Physics Division, Oak Ridge National Laboratory, Oak Ridge, TN 37831, USA;*
*13. Flerov Laboratory for Nuclear Reactions, JINR, Dubna 141980, Russia;*
*14. Lawrence Livermore National Laboratory, Livermore, CA 94550, USA;*
*15. Instituto de Fisica, Facultad de Ingenieria, C.C. 30, 11300 Montevideo, Uruguay;*
*16. Physics Department, Mississippi State University, Mississippi State, MS 39762, USA;*)

**Abstract:** This paper reviews the systematic investigations and understanding for the shape transitions and coexistence with regard to triaxial deformations in $A \sim 100$ to 126 neutron-rich Rh ($Z = 45$), Pd ($Z = 46$), Ag ($Z = 47$), Cd ($Z = 48$) and Zr ($Z = 40$), Nb ($Z = 41$), Mo ($Z = 42$), Tc ($Z = 43$) isotopes with $Z$ beyond and below Ru ($Z = 44$), respectively, in Ru the maximal triaxial deformation having been predicted and deduced. The recent measurements and studies of prompt triple- and four-fold, γ-γ-γ and γ-γ-γ-γ, coincidence data from the spontaneous fission of $^{252}$Cf using Gammasphere have yielded considerable expansion and extension or first observation of the bands in Ru, Pd, Cd, and Nb isotopes, which provided important data for the studies of nuclear shapes in this region. Combined with previous investigations, recent systematic studies of the new data well reproduced by PES, TRS, PSM, CCCSM

**Received date:** 1 Sep. 2014; **Revised date:** 24 Nov. 2014

**Foundation item:** US Department of Energy(DE-FG-05-88ER40407, DE-AC02-05CH11231, DE-FG02-95ER40934, DE-AC05-00OR22725, DE-AC52-07NA27344, DE-FG02-95ER40939); National Natural Science Foundation of China (11175095, 10975082, 11235001, 11320101004, 11305059, 11275063, 11275068, 11135005, 11075103); Special Program of Higher Education Science Foundation(2010000211007); National Basic Research Program of China(973 Program)(2013CB834401); Russian Foundation for Basic Research (11-02-12050, 11-02-12066)

**Biography:** LUO Yixiao(1944–), male(Han Nationality), Zigong, Sichuan, Researcher, working on nuclear structure;
E-mail: yxluo@lbl.gov.

and SCTAC model calculations have traced shape changes along the isotonic and isotopic chains, respectively, and with changing excitations/spins as well, significantly expanding our knowledge of shape transitions/coexistence in nuclei.

For the neutron-rich Ru and beyond, Rh, Pd, Ag and Cd isotopes, triaxial deformations $\gamma = -28°$, slightly smaller than the maximal value, were deduced in Rh ($Z = 45$) isotopes, with chiral symmetry breaking proposed in $^{103-106}$Rh; onset of wobbling motions were identified in $^{112}$Ru and $^{114}$Pd ($N = 68$), and probably also in $^{114}$Ru ($N = 70$); evolution from chiral symmetry breaking in $^{110,112}$Ru with maximal triaxial deformations to disturbed chirality in $^{112,114,116}$Pd with less pronounced triaxial deformations was proposed; rich nuclear structure was proposed in soft Ag isotopes with possible chiral doubling structure suggested in $^{104,105}$Ag, and softness towards triaxial deformation proposed in heavier $^{115,117}$Ag; quasi-particle couplings, quasi-rotations and soft triaxiality were suggested in Cd ($Z = 48$) isotopes with small deformations; onset of collectivity was recently suggested in $^{122,124,126}$Cd in the vicinity of $Z = 50$ and $N = 82$ closed shells by studies of Coulomb excitations; shape evolutions from maximal triaxial deformations in Ru ($\gamma = -30°$, with triaxial minimum energy gain of 0.67 MeV), through Rh with large triaxial deformations ($\gamma = -28°$), to less pronounced triaxiality in Pd (with triaxial minimum energy gain of 0.32 MeV), then soft triaxiality in Ag, and finally to slightly deformed Cd isotopes but with emergence of collectivity and soft triaxiality were proposed. The systematic studies of the band crossings in Pd revealed up-rising $\gamma$ drivings of the first band crossings caused by $(\nu h_{11/2})^2$ and down-sloping $\gamma$ drivings of the second band crossings by $(\pi g_{9/2})^2$, explained the onset of wobbling motions in $^{114}$Pd, and showed a long-sought picture of shape evolution and coexistence in the Pd isotopic chain which is more complete but complex than earlier predictions. Based on the systematic studies in the mass region, maximal triaxial deformation is found to be reached in $^{112}$Ru and less-pronounced triaxiality centered at $^{114}$Pd, both for $N = 68$, four neutrons more than predicted in earlier theoretical calculations.

In the neutron-rich Zr ($Z = 40$), Nb ($Z = 41$), Mo ($Z = 42$) and Tc ($Z = 43$) isotopes with $Z$ just below Ru, large quadrupole deformations of axially symmetric shapes were deduced in Y and Zr isotopes, with emergence of the $\gamma$ degree of freedom having been suggested for heavier Zr isotopes; medium triaxial deformations were deduced for the ground states of heavier ($A \geqslant 104$) Nb isotopes, and, with increasing excitations and spins, evolution from medium triaxial deformations with strong quadrupole deformations at ground states to nearly axially-symmetric shapes were deduced; light Nb isotopes ($A \leqslant 103$) have near axially-symmetric shapes with strong quadrupole deformations; combining with the identification of onset of strong quadrupole deformation at $^{100}$Nb in the Nb isotopic chain, an increase of soft triaxiality with increasing neutron number was proposed in $^{100-106}$Nb. Shape coexistence with regard to soft triaxiality is also proposed in Nb isotopes; large triaxial deformations, $\gamma$ vibrations and chiral doublets were proposed in Mo isotopes; chiral doubling and large triaxial deformations ($\gamma \sim -26°$) slightly smaller than the maximal triaxiality were suggested in Tc isotopes.

The neutron-rich nuclei with $Z$ ranging from 41 through 48 and $A \sim 100$ to 126, especially the Pd and Nb isotopes are thus found to be transitional nuclei with regard to triaxiality.

**Key words:** neutron-rich nuclei with $Z$ from $Z = 41$ through $Z = 48$; nuclear shape transition and coexistence; prolate-to-oblate shape transition; triaxial deformation; triaxial wobbling motion; chirality; disturbed chirality; $\gamma$ vibrational band; high-spin states; band crossing; $\gamma$ driving, quasi-rotation; onset of collectivity and soft triaxiality in the vicinity of $Z = 50$ and $N = 82$ closed shells; level scheme; spin/parity/configuration assignment, PES, PSM, TRS, CCCSM and SCTAC model calculations; prompt $\gamma$ spectroscopy based on spontaneous fission; $\gamma$-$\gamma$-$\gamma$; $\gamma$-$\gamma$-$\gamma$-$\gamma$ and $\gamma$-$\gamma$ ($\theta$) coincidences; $^{252}$Cf; multi-detector array Gammasphere

**CLC number:** O571.21 **Document code:** A **DOI:** 10.11804/NuclPhysRev.32.01.001

## 1 Introduction

The neutron-rich nuclei with $A \sim 100$ to 126 over long isotonic and isotopic chains in Zr ($Z = 40$), Nb ($Z = 41$), Mo ($Z = 42$), Tc ($Z = 43$), Ru ($Z = 44$), Rh ($Z = 45$), Pd ($Z = 46$), Ag ($Z = 47$) and Cd ($Z = 48$) are intermediate between the spherical doubly magic $^{132}$Sn and the strongly deformed axially symmetric Sr ($Z = 38$), Y ($Z = 39$) isotopes to exhibit an increasing richness of nuclear structure and shapes[1–4]. For the nuclei in this region, the Fermi level relative to the high-j subshells, $\nu h_{11/2}$ and $\pi g_{9/2}$, ranges from the bottom of the shells, through the near middle (half filled) shells to upper half of the shells, favoring prolate (or triaxial prolate), through large triaxial deformations

to oblate (or triaxial oblate) shapes, respectively. This nuclear region is characteristic of shape transitions and coexistence and provides good opportunities for searching and studying the predicted shape changes and new excitations with regard to triaxial deformations[5–12].

The studies of nuclear shapes have long been one of the hot topics in the investigations of nuclear structure[13–18]. All nuclei were initially considered to have spherical shapes. When well-deformed ground states were observed in rare earth and actinide nuclei, they all were found to have prolate shapes, as described in the Bohr-Mottelson Model[13]. The observations that about 86 percent of the nuclides are prolate were explained by analyzing the properties of the Nilsson potential[19].

However, oblate shapes and triaxial axially-asymmetric shapes were found and are receiving more and more attention. Triaxial shapes could be based on either prolate or oblate shapes. Early on searches for nuclear ground states with oblate or triaxial shapes had little if any success. Early inklings for oblate shapes came from nuclei around $^{72}$Se and $^{74}$Kr where nuclear shape coexistence was found in 1974[15] and 1981[16], respectively. In these cases the ground states and states built on them were found to have near spherical or oblate shapes with other excited states built on strongly deformed prolate shapes in $^{72}$Se and the reverse in $^{74}$Kr with a strongly deformed prolate ground state. Comparisons of the most recent theoretical calculations with experimental data reproduce the two coexisting shapes in these two nuclei. The importance of triaxial shapes in the coexistence of the two shapes is found along with a ground state shape transition from oblate in $^{72}$Kr to prolate in $^{74,76}$Kr. While approaching the proton drip line in the $A\sim80$ and $A\sim190$ mass region, coexisting prolate-oblate shapes were found[20].

Various theoretical calculations were carried out in the 1990s predicting a similar, but reverse, prolate-to-oblate ground state shape transition as the neutron number increased in neutron-rich $^{107–114}$Ru and $^{108–116}$Pd[18,21]. The theoretical calculations of Hartree-Fock energy surfaces for low-lying states in Ru suggested an evolution from near prolate to triaxial in $^{108,110,112}$Ru[22]. The cranked- and configuration-constrained shell model (CCCSM) calculations[5] show that with increasing neutron number in the $Z\geqslant40$ region nuclear shapes evolve from prolate through triaxial to oblate for $N\geqslant70$, and the oblate shapes dominate over a wide spin range. Global theoretical calculations of nuclear shapes throughout the Chart of Nuclides[17] predicted that $^{108}$Ru, which has the deepest potential well for a triaxial shape, is the center of the region of triaxial deformations, and a large but less pronounced potential well was calculated in $^{110}$Pd. Chiral symmetry breaking was predicted to occur in the nuclei with large and stable triaxial deformations[23].

For a long period of time, the predicted shape transitions with increasing neutron numbers in Pd remained unconfirmed by experiments. Studies of high spin states in $^{109–112}$Ru were interpreted as due to a triaxial shape transition from prolate to oblate occurring in $^{111}$Ru. The new experimental studies of $^{108,110,112,114}$Ru identified odd-parity doublet bands interpreted as chiral symmetry breaking in $^{110,112}$Ru[23–24], and established $^{110,112}$Ru as more rigid triaxial rotors with $^{108}$Ru having a more soft structure. Chiral doublets were also reported in $^{103–106}$Rh (*e.g.* Ref. [25]), although their triaxial deformations were deduced to be slightly smaller than the maximal value[9]. The experimental observations and interpretations of the one- and two- phonon $\gamma$ vibrational bands in the Ru and Pd isotopes provided the earlier information for triaxial deformations in these isotopes[3, 26–28]. The evolution of triaxiality at high spins has been addressed by lifetime measurements[29].

Recently, energy levels in $^{112–118}$Pd were investigated in greater detail[30]. In addition to the search for possible chiral symmetry breaking in Pd isotopes, searches for wobbling motions in Ru and Pd isotopes, especially in the isotopes around $N=68$ isotones $^{112}$Ru and $^{114}$Pd, were performed[30], since wobbling motions were also predicted for well deformed triaxial nuclei[31–33].

The recent study of the systematics of the intriguing band-crossings in Pd isotopes by total Routhian surface (TRS) calculations provided a more complete but complex picture of shape transitions than previous predictions, which are closely related to evolutions of triaxial deformations[30].

The studies of the band structures of $^{104–117}$Ag over a wide isotopic chain yielded rich structural information such as softness towards triaxiality[34], possible chiral doubling[35–36], magnetic rotations[37–38], band structure reproduced by microscopic triaxial projected shell model[39], and change of rotation axis[40–41].

For Cd ($Z=48$) isotopes with only two proton holes in the $Z=50$ major shell, a number of model calculations suggested spherical-vibrational structure, quasi-particle couplings, quadruple-octupole couplings (QOC), soft triaxial deformations and so on (*e.g.* Refs. [11-12, 42]). Considerable disagreements in interpretations for the structure of the Cd isotopes remain as open questions (*e.g.* Ref. [42]). In order to gain new insight into the shapes and structure of the Cd isotopes, energy levels and new bands of Cd isotopes

were recently expanded and extended[43]. The shell-correction tilted-axis-cranking model (SCTAC)[44-45] applied for near spherical nuclei was used for the Cd isotopes to study their triaxiality and collectivity from a new point of view. A very recent study of Coulomb excitations of heavy $^{122,124,126}$Cd measured the reduced transition probability and limits for quadrupole moments of the first $2^+$ excited states, suggesting onset of collectivity in the vicinity of $Z = 50$ and $N = 82$ closed shells[46].

For the neutron-rich nuclei with $Z$ below Ru, axially-symmetric shapes with strong quadrupole deformations, $\varepsilon_2 = 0.39 \sim 0.41$, were identified in Y($Z = 39$)[4], and moderate quadrupole deformations and large triaxial deformations slightly smaller than the maximal triaxiality were deduced in Tc ($Z = 43$) isotopes[10]. The Zr ($Z = 40$) isotopes were believed to be axially symmetric with strong quadruple deformations (*e.g.* Ref. [47]), but very recently further work suggested the emerging of triaxiality in the heavier Zr isotopes[48]. Level schemes were extended and expanded and $\gamma$ vibrational bands were proposed in $^{104\text{-}106,108}$Mo[49–53]. Triaxial deformations and chiral doubling were suggested in $^{106,108}$Mo ($Z = 42$) isotopes[7, 54]. For Nb ($Z = 41$) isotopes, collective bands with large quadrupole deformations were established in $^{101–105}$Nb[4, 55–57]. They were also found to have small to medium triaxial deformations ($\gamma \sim -5°$ to $-19°$)[4]. With increasing neutron number, a sudden shape transition from spherical to large quadrupole deformation in the Nb isotopic chain was found to take place at $N = 59$ in $^{100}$Nb[58], in contrast to $N = 60$ for Sr ($Z = 38$), Y ($Z = 39$), Zr ($Z = 40$) and Mo ($Z = 42$) isotopes. New experimental and theoretical efforts were recently pursued to explore heavier, more neutron-rich Nb isotopes, especially odd-odd Nb isotopes[59], and these efforts yielded detailed results on triaxial shape evolutions.

This paper will combine the previous and recent progress to review the shape transition/coexistence with regard to triaxial deformations in the isotopes with $Z$ beyond and below Ru, respectively, with a focus on the recent achievements in the experimental and theoretical studies of triaxial shape changes in Ru, Pd, Cd and Nb isotopes. The studies of shape changes in Ru - Pd isotopes were mainly based on the search and discovery of wobbling motions and chirality, and on the reproductions of the intriguing band-crossings observed in Pd isotopes by TRS calculations[30]. The study of Cd isotopes was based on the level systematics and reproductions of the band crossings by SCTAC model[43] and, very recently, on study of the Coulomb excitations[46]. The shape transitions in Nb isotopes were studied by fitting the level structures of $^{104,106}$Nb, the odd-odd Nb isotopes so far identified, by potential energy surface (PES) and projected shell model (PSM) calculations[59]. The even-N $^{103,105}$Nb were recently re-studied. One-phonon and two-phonon vibrational bands were identified to provide additional information concerning triaxiality in the Nb isotopic chain[60–61]. TRS calculations were recently carried out to provide further information of soft triaxial shape evolution and coexistence in $^{101,103}$Nb.

The publications reviewed in this paper have adopted different conventions for the triaxial shape parameter $\gamma$. As a measure of the degree of triaxiality of a nucleus, $\gamma = 0°$ represents a prolate shape and $\gamma = -60°$ an oblate shape and $\gamma = -30°$ or $+30°$ maximum triaxiality, the negative (positive) $\gamma$ value in the later giving more (less) collective triaxiality.

## 2 Experiments and new efforts in experimental data analysis for the related weakly populated bands in this nuclear region

Prompt fission $\gamma$ rays from spontaneous fission, fusion-fission and induced fission, decay $\gamma$s from fission fragments, and Coulomb excitations at radioactive ion-beam facility were used for the experimental studies of the related neutron-rich nuclei. The prompt fission $\gamma$ rays from partner isotopes populated in spontaneous fission and detected by multi-detector arrays have proven to be a "gold mine" for the production and studies of low- to high-spin states of neutron-rich nuclei[62], and played the most important role in the studies of the nuclei in this nuclear region. From experiments and data-analysis points of view, this paper reviews mainly the new experimental efforts in the systematic searches and studies of the related weakly-populated bands of Ru, Pd, Cd and Nb isotopes by means of measurements of prompt fission $\gamma$ rays from spontaneous fission of $^{252}$Cf by Gammasphere.

Over $5.7 \times 10^{11}$ triple-fold, $1.9 \times 10^{11}$ four-fold and higher-fold coincidence events, factors of $10 \sim 100$ higher than earlier measurements, were accumulated by Gammasphere[63]. Less-compressed data cubes were used with new Radware programs of a decade ago[64]. The recently constructed triple-gated 4d hypercube data with such a high event accumulation turned out to be very powerful in exploring weakly-populated levels. The details of experiment and data analysis for the prompt fission $\gamma$ rays can be found in previous publications, *e.g.*, a review paper Ref. [54].

Fifteen new high-spin level schemes of $^{112,114–118}$Pd[30], $^{117–120,122}$Cd[43], $^{104,106}$Nb[59], and

$^{103,105}$Nb[60–61] were established. These were considerably extended and expanded by means of γ-γ-γ, γ-γ ($\theta$) and γ-γ-γ-γ measurements. The level scheme of $^{106}$Nb was proposed for the first time[59].

Fig. 1 shows an example of the cross-checking triple-gated quadruple-coincidence spectra created in the data analysis for the first observation of the weakly-populated odd-parity doublet bands in $^{114}$Pd[30]. The weakly-populated doublet bands of $^{112,114,116}$Pd exhibit very small intensities in the spectra due to the weak populations and rich decay-out paths, the later of which make the coincident peak areas even smaller, no matter how one sets the gates. It was also the serious peak overlapping of the band members with low-lying strong transitions that prevented the doublet bands being identified. However, triple-gating with the 4d data which have such a high event accumulation provided convincing evidence to identify these bands. In Fig. 1 one can see the excellent resolution and cleanness, peak-to-total ratio and FWHM of the peaks. Another triple-gated spectrum is shown in Fig. 2 for data analysis of the weakly populated band in odd-odd $^{106}$Nb[59]. It is worth noting that for fission data analysis with gates set in the energy region such as those in Fig. 2, there are serious contaminations and peak overlapping due to contaminations of gates in the double-gated spectra. However, it can be seen in Fig. 2 that the triple-gated spectrum is clean enough, providing clear evidence for the identification of the weakly-populated bands.

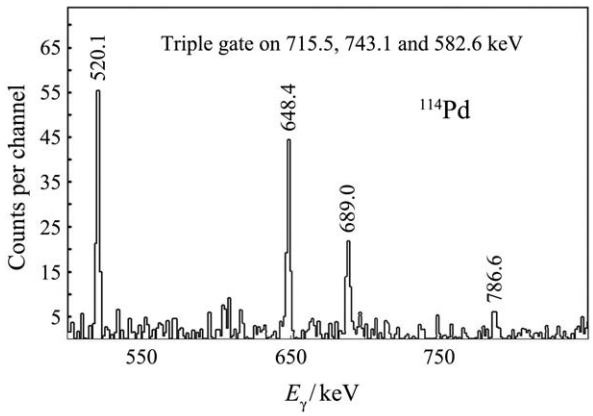


Fig. 1　Excellent resolution and cleanness, peak-to-total ratios and FWHM seen in a triple-gated quadruple-coincidence spectrum based on the 4d hypercube fission data, showing evidence for the first observation of the very weakly populated (see the counts of the full scale) but well-extended band 7 of the odd-parity doublet bands in $^{114}$Pd, which was interpreted as disturbed chiral doublet bands in the nucleus with large but less pronounced triaxial deformation than that of $^{112}$Ru[30] (also see Fig. 3).

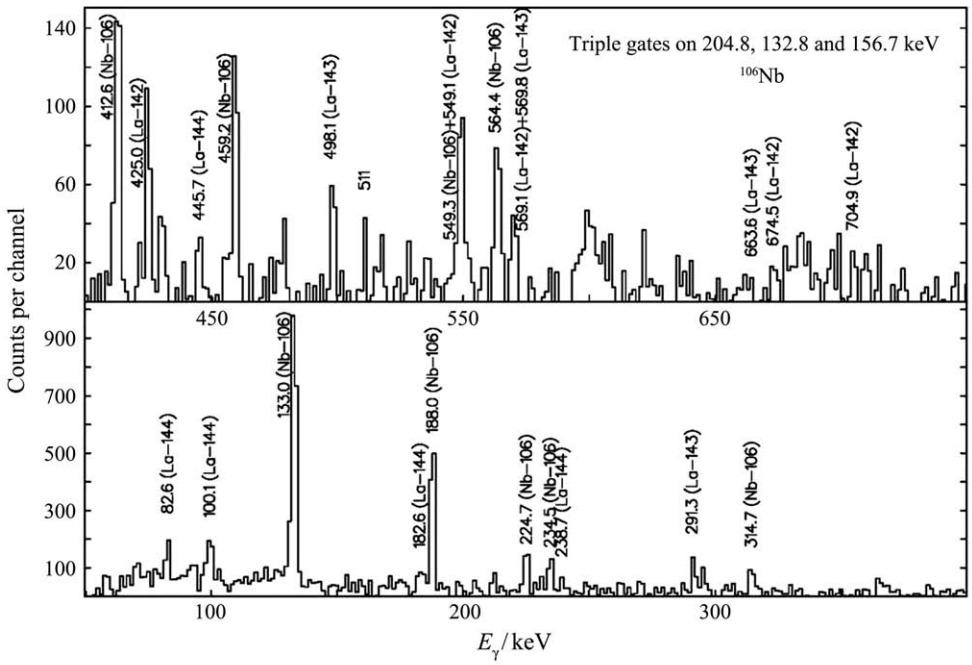


Fig. 2　A triple-gated spectrum with gates set in an energy region where the gate-contaminations in double-gating would cause serious contaminations and possibly also peak overlapping. However, the excellent resolution, peak-to-total ratio, FWHM and comparatively good cleanness were achieved in the triple-gated quadruple-coincidence spectrum based on the 4d hypercube data, showing clear evidence for the first observation of the weakly-populated but well-extended band of $^{106}$Nb[59] (see Fig. 14).

Angular correlation, $\gamma$-$\gamma$ ($\theta$), measurements as described by Daniel *et al.*[65] were made to provide basic information for the spin/parity assignments for some levels, mainly for the doublet bands observed in $^{112,114,116}$Pd, levels in $^{115,118}$Pd[30], and those in Cd isotopes[43]. Shown in Table 1 are the angular correlations for some key transitions in the Pd isotopes. Spin changes and multipolarities of the transitions deduced were indicated in the table. Considering also the decay pattern, spins and odd-parity were assigned to the levels of $^{112,114,116,118}$Pd, mainly for the doublets. The spin/parity assignments for Nb isotopes were based on PES and PSM calculations[59].

Table 1 Angular correlations measured for some key transitions of $^{112,114,116,118}$Pd and $^{115}$Pd[30]. The theoretical $A_2$, $A_4$ and $\delta$ were taken from[66–67].

| Nucleus | Level (keV) to be assigned | Cascade /keV | $(A_2/A_0)^{\rm exper.}$ | $(A_2/A_0)^{\rm Theor.}$ | $(A_4/A_0)^{\rm exper.}$ | $(A_4/A_0)^{\rm Theor.}$ | $\delta^{\rm Theor.}$ | Spins of cascade | Spin change and multiplarity |
|---|---|---|---|---|---|---|---|---|---|
| $^{112}$Pd | 2704.9 | 1154.0–667.7 | −0.074(21) | −0.071 | 0.011(32) | 0.000 | 0.00 | 7 − 6 − 4 | 1, pure dipole |
| | 2711.3 | 1160.4–667.7 | −0.098(37) | −0.071 | 0.008(57) | 0.000 | 0.00 | 7 − 6 − 4 | 1, pure dipole |
| $^{114}$Pd | 2184.6 | 1331.7–332.8 | −0.067(15) | −0.071 | 0.004(23) | −0.000 | 0.00 | 5–4 . . . 2–0 | 1, pure dipole |
| | 2599.3 | 1098.0–332.8 | −0.069(10) | −0.071 | 0.035(15) | −0.000 | 0.00 | 7–6 . . . 2–0 | 1, pure dipole |
| | 2790.1 | 1288.8–648.4 | −0.079(16) | −0.071 | 0.032(24) | −0.000 | 0.00 | 7 − 6 − 4 | 1, pure dipole |
| | | 1288.8–520.1 | −0.069(19) | −0.071 | 0.024(29) | −0.000 | 0.00 | 7–6 . . . 4–2 | 1, pure dipole |
| | 3239.0 | 1022.2–520.1 | −0.059(36) | −0.071 | −0.019(55) | 0.000 | 0.00 | 9–8 . . . 4–2 | 1, pure dipole |
| $^{116}$Pd | 1983.9 | 1105.8–537.6 | −0.064(12) | −0.071 | −0.005(18) | −0.000 | 0.00 | 5 − 4 − 2 | 1, pure dipole |
| | 2436.8 | 877.0 − 681.7 | −0.078(16) | −0.071 | 0.025(25) | −0.000 | 0.00 | 7 − 6 − 4 | 1, pure dipole |
| | 2655.7 | 1095.9–681.7 | −0.077(74) | −0.071 | −0.129(144) | −0.000 | 0.00 | 7 − 6 − 4 | 1, pure dipole |
| $^{118}$Pd | 2493.0 | 821.4 − 718.3 | 0.146(95) | 0.102 | 0.127(145) | 0.009 | 0.00 | 8 − 6 − 4 | 2, E2-E2 |
| $^{115}$Pd | | 340.5 − 488.9 | 0.128(27) | 0.102 | 0.016(42) | 0.009 | 0.00 | 11/2 − 7/2 − 3/2 | 2, E2-E2 |
| | | 743.5 − 394.8 | 0.080(18) | 0.102 | 0.036(27) | 0.009 | 0.00 | 23/2 . . . 15/2−11/2 | 2, E2-E2 |
| | | 579.9 − 394.8 | 0.097(15) | 0.102 | 0.045(23) | 0.009 | 0.00 | 19/2 − 15/2−11/2 | 2, E2-E2 |
| | | 642.6 − 530.5 | 0.068(48) | 0.102 | 0.036(75) | 0.009 | 0.00 | 17/2 − 13/2 − 9/2 | 2, E2-E2 |

New level schemes of $^{112,114–118}$Pd[30], $^{117–120,122}$Cd[43], odd-odds $^{104,106}$Nb[59] and $^{103,105}$Nb[60–61] were established based on the coincident relationships, relative intensities and, if available, on angular correlations and/or model reproductions.

## 3 Theoretical interpretations and discussions: the shape transitions and coexistence with regard to triaxiality in nuclei with $Z$ beyond and below Ru, respectively, where maximal triaxial deformation was predicted and deduced

### 3.1 The shape transitions and coexistence with regard to triaxiality in Rh, Pd, Ag and Cd with $Z$ beyond Ru

The detailed studies of Rh ($Z$ = 45) isotopes revealed a medium quadrupole deformations $\varepsilon_2$ = 0.27 ∼ 0.28 and triaxial deformations $\gamma = -28°$ slightly smaller and near the maximal value of triaxiality[9]. Chiral symmetry breaking was proposed in $^{103–106}$Rh[25]. The large and slightly decreased triaxial deformations in Rh in comparison to the maximal triaxiality in Ru support the predictions in Ref. [17].

Very rich structural information was reported in $^{104–117}$Ag, a long isotopic chain: softness towards triaxiality in $^{115,117}$Ag[34], possible chiral doubling structure in $^{104,105}$Ag[35–36]; magnetic rotations in $^{106,107}$Ag[37–38]; band structure of $^{108}$Ag well reproduced by microscopic triaxial projected shell model calculations[39], change of rotation axis in Ag isotopes[40], and principal axis rotation in $^{109,110}$Ag described by a model with two quasiparticles coupled to triaxially deformed core[41]. For the study of chirality it is worth mentioning that the previously suggested $\gamma$-soft shape in $^{106}$Ag[68] was found to change to more $\gamma$-rigid axially-symmetric shapes in the yrast levels of $^{105}$Ag, and, instead, a newly observed pair of bands

with weak populations was identified as possible chiral doublet bands[35]. This progress and clarification are convincing because the strongly populated bands with the yrast band involved are not likely chiral, since the triaxial deformations in these Ag isotopes are considerably smaller and soft.

After the identifications of chiral symmetry breaking in $^{110,112}$Ru[24], searches for possible chiral doublets and studies of the chirality in the Pd isotopes, especially in the isotopes around the $N = 68$ isotone $^{114}$Pd, were intensively carried out[30]. Since wobbling motion was also predicted in triaxial nuclei[31–33], special attention was paid to search for wobbling motions in Ru and Pd isotopes as well. The efforts provided significant information showing the shape changes with regard to triaxial deformations in Ru-Pd isotopes.

Fig. 3 depicts the new partial level scheme of $^{114}$Pd, an example of those of $^{112,114,116}$Pd, in which the extended $\gamma$ bands and first observations of odd-parity doublet bands serve as important data for the search of wobbling motions and chirality (see 3.1.1 and 3.1.2). The extension of the ground band offers key data for interpretation of a second band crossing in the isotope. The establishment of the systematic band crossings in Pd isotopes reproduced by TRS calculations revealed the long-sought shape evolutions in Pd isotopes. Fig. 4 shows the new level scheme of $^{115}$Pd. Note that following the previous work on $^{115}$Pd[69-73] the extension of band 2 consists of three newly identified transitions 870.1, 854.2 and 867.6 keV with energies very close to each other. The extensions of bands 1 ($\nu h_{11/2}$ band) and 2 ($\nu g_{7/2}$ band) confirmed the absence of the first band-crossing in band 1 and the occurrence of a second crossing in band 2, respectively, providing key experimental data for the shape coexistence deduced in the nucleus.

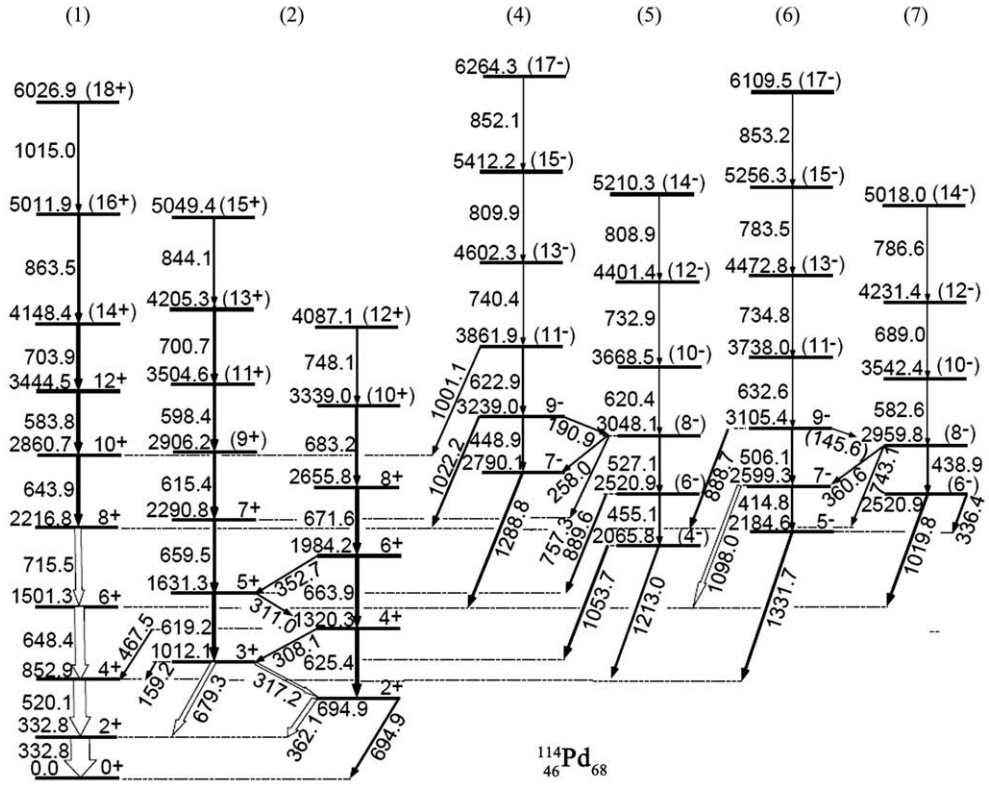


Fig. 3　New partial level scheme of $^{114}$Pd[30] including only the ground-state band (band 1), $\gamma$ band (band 2) and odd-parity doublet bands (band $4 \sim 7$). The weakly populated odd-parity doublet bands are identified for the first time, and found to extend to excitations even higher than that of the ground-state band. The doublet bands exhibit good energy degeneracy (see the following Fig. 7) and seems similar to those observed in the triaxial chiral $^{110,112}$Ru. However, the level staggerings in the doublet band imply disturbance for the chirality (see the following Fig. 8). The level staggering in the extended $\gamma$ band, band 2, provided evidence for triaxial wobbling motion in the nucleus, as proposed in the first even-even wobbler $^{112}$Ru[31] (see the following Fig. 6). Odd-parity doublet bands, extended $\gamma$ bands and ground bands were also established in $^{116}$Pd and $^{112}$Pd, which look similar to those of $^{114}$Pd, except for the different behavior of band-crossing of the ground bands and staggering of the $\gamma$ bands[30].

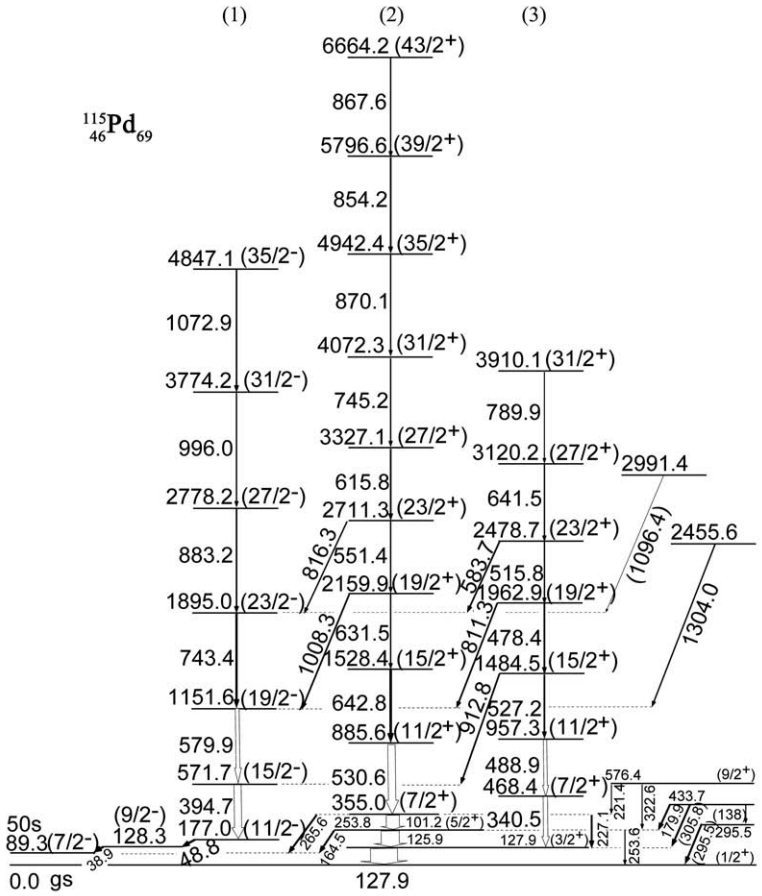


Fig. 4 New level scheme of $^{115}$Pd[30]. The extensions of the bands are the key to deducing shape coexistence in the nucleus. See text in subsection 3.1.3.

### 3.1.1 Searches and studies of triaxial wobbling motions in neutron-rich Ru and Pd isotopes: the identifications of the onset of wobbling motions in $^{112}$Ru and $^{114}$Pd, the $N = 68$ isotones, likely also in $^{114}$Ru ($N = 70$); and the evolution of wobbling motions and triaxiality with changing neutron number and spins

The wobbling motions predicted in a triaxial nucleus constitute a revolving motion of $J$ about an axis of a triaxial nucleus[31–33] (Fig. 5), and have been reported in $^{161,163,165,167}$Lu and $^{167}$Ta at high spins(*e.g.* Ref. [74]). Wobbling motions are expected to occur at moderate spins if the predicted triaxial shapes lead to different moments of inertia for the three principal axes. Wobbling motion manifests itself as a fingerprint that the excitations of the $\alpha = 0$ wobbling (even-spin members of the $\gamma$ band) are above those of the $\alpha = 1$ wobbling (odd-spin members of the $\gamma$ band) in an even-even nucleus[30–32].

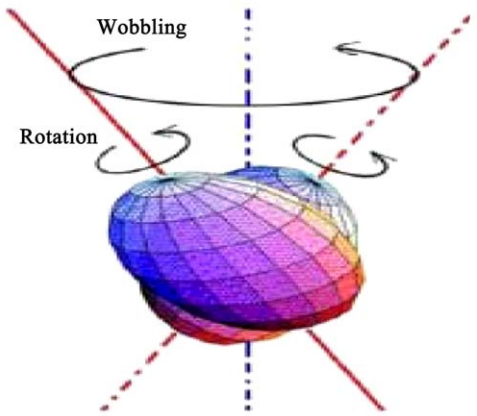


Fig. 5 (color online) Wobbling motion predicted in a triaxial nucleus: a revolving motion of $J$ about an axis of the triaxial nucleus. Wobbling motion manifests itself as the staggering in the $\gamma$ band, namely the relative excitations of the even-spin members and odd-spin members of the $\gamma$ vibrational band of the nucleus. See text.

Based on the extended $\gamma$ bands, bands 2, in the $N = 64 \sim 70$ Ru and Pd isotones[3, 27, 30, 75] (see the level scheme of $^{114}$Pd in Fig. 3), excitation energies of the levels are plotted against spins in Fig. 6. As can be seen in the figure, in $^{110}$Ru and $^{112}$Pd ($N = 66$

isotones) no wobbling motion is seen until spin ∼6 and 10, respectively [Fig. 6(a)]. Onset of wobbling motion takes place in $^{112}$Ru and $^{114}$Pd ($N=68$ isotones) [Fig. 6(b)]. So, following the identification of the first even-even wobbler $^{112}$Ru[31], the $N=68$ isotone $^{114}$Pd was found to be another even-even wobbler at low to medium spins[30]. Wobbling motions are likely also seen in $^{114}$Ru ($N=70$) [Fig. 6(c)] although the separations of the two curves of $^{114}$Ru in the plot are smaller than those of $^{112}$Ru, which may imply smaller triaxial deformations in $^{114}$Ru than those in $^{112}$Ru, and even smaller separations can be seen in $^{116}$Pd, consistent with the calculations of Möller, *et al.*[17]. While going back to lighter $N=64$ isotones $^{108}$Ru and $^{110}$Pd [see Fig. 6(d)], no wobbling motions are confirmed in the whole spin region observed. The studies of the $N=64\sim70$ Ru and Pd isotones thus indicate an evolution and onset of wobbling motions in $N=66\sim70$ Ru and Pd isotones as follows: For $N=64$, no wobbling motions; for $N=66$, no wobbling motions until spin ∼6 and 10, respectively; for $N=68$, early onsets of wobbling motions take place; and for $N=70$, wobbling motions are likely also seen in $^{114}$Ru but with smaller separations (level staggering). It is worth noting some details of the results of related work on $^{114}$Ru. A large triaxial deformation of $\gamma=27.2°$ was calculated for the ground state of $^{114}$Ru by rigid triaxial rotor (RTR) model[27]. In a recent study of $^{114}$Ru[75], both the cranked shell model calculations for the extended ground band and the TPSM calculations for the extended and expanded $\gamma$ vibrational bands suggested a similar triaxial deformation $\gamma=27°$ for this nucleus.

The above observations and the deduced evolutions of wobbling motions trace the triaxial shape changes along the Ru and Pd isotopic chain, respectively.

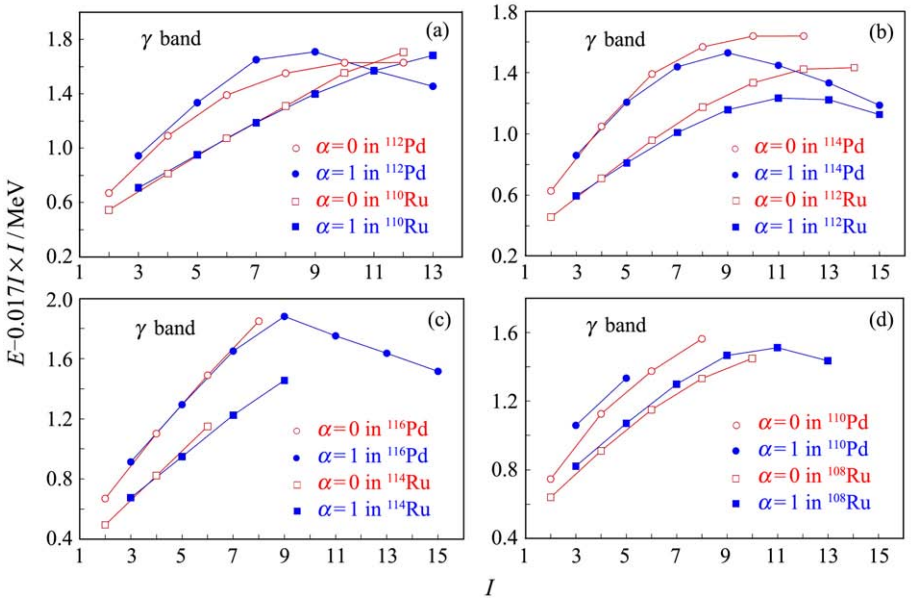


Fig. 6 (color online) Excitation energies of the $\gamma$ band plotted against spin for $N=66$ isotones $^{110}$Ru and $^{112}$Pd (a); $N=68$ isotones $^{112}$Ru and $^{114}$Pd (b); $N=70$ isotones $^{114}$Ru and $^{116}$Pd (c) and, back to $N=64$ isotones $^{108}$Ru and $^{110}$Pd (d). Based on the relative locations, the crossing points and separations (level staggering) of the $\alpha=0$ wobbling and the $\alpha=1$ wobbling, fingerprints of the wobbling motions are checked and the evolution and onset of the wobbling motions in Ru and Pd isotones are identified. See text.

### 3.1.2 Searches and studies of possible chiral symmetry breaking in Pd isotopes; the evolution from disturbed chirality in $^{112,114,116}$Pd with less-pronounced triaxiality to chiral $^{110,112}$Ru with maximal triaxiality, as also seen from γ-soft $^{108}$Ru to chiral $^{110,112}$Ru

The characteristic conditions for generating chirality[24], and all the fingerprints for chiral symmetry breaking are seen in the doublet bands in $^{110,112}$Ru: A. The partner levels (levels with the same spin/parity) are nearly degenerate in energy (see Fig. 7). B. The partner levels have very similar electromagnetic properties, their $B(\mathrm{E2})/B(\mathrm{M1})$ ratios being consistent with each other within error limits. C. Their energy-staggering parameter $S(I)$ values are nearly equal and constant with spin (Fig. 8). These features were explained by tilted-axis-cranking (TAC) calculations.

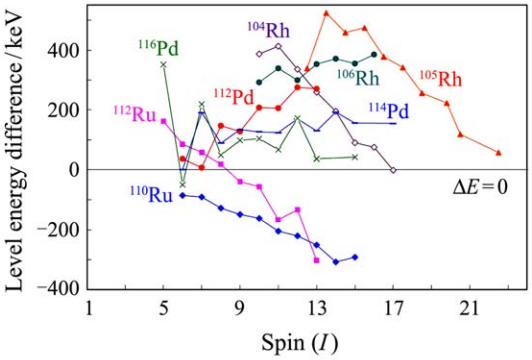


Fig. 7 (color online) Energy degeneracy of the partner levels of the doublet bands in $^{110,112}$Ru and $^{112,114,116}$Pd. Also shown in the figure are those of the previously reported chiral nuclei. Very good energy degeneracy is seen in the doublet bands of $^{112,114,116}$Pd.

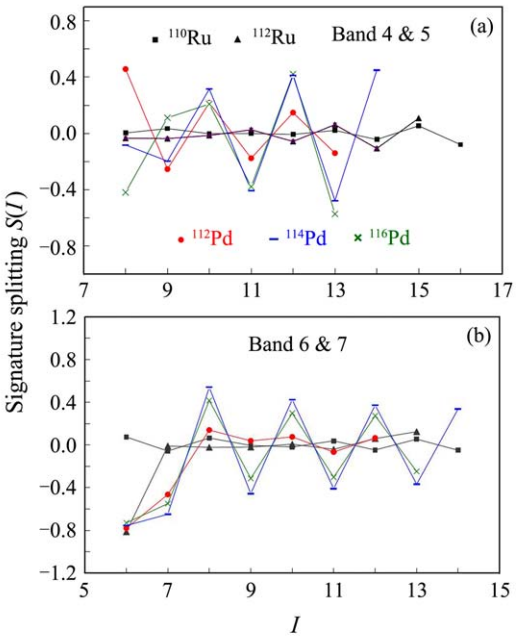


Fig. 8 (color online) Large level staggering observed in the doublet bands of $^{112,114,116}$Pd[30], as seen in the $\gamma$-soft $^{108}$Ru, in contrast to the small and nearly constant $S(I)$ with spin in $^{110,112}$Ru[24], as expected for chiral symmetry breaking. The big level staggering in the doublet bands of $^{112,114,116}$Pd do not fulfill the $S(I)$ criterion for chiral symmetry breaking. Note that the triaxial minimum energy gain of 0.67 MeV is predicted in $^{108}$Ru but a considerably smaller one of 0.32 MeV in $^{110}$Pd[17, 33]. See text below.

The doublets in $^{110,112}$Ru are zero- and one- phonon chiral vibration bands built on a $\nu h_{11/2}\times(d_{5/2}g_{7/2})^{-1}$ configuration, giving odd-parity. The search and studies in Pd isotopes have yielded interesting results. In $^{114}$Pd, the $N = 68$ isotone of $^{112}$Ru, the weakly-populated doublet bands extend to excitations even higher than that of the ground-state band (see Fig. 3), implying smaller level density in the potential well where the bands are built in. However, while the odd-parity doublet bands observed in $^{112,114,116}$Pd[30], especially the doublets in $^{114}$Pd, exhibit good energy degeneracy (see Fig. 7), they show dramatic level staggering, as also observed in the doublet bands of $^{108}$Ru[24]. One can see that the large staggerings in $^{112,114,116}$Pd in Fig. 8, as observed in the $\gamma$-soft $^{108}$Ru, do not fulfill the $S(I)$ criterion, implying disturbed chirality in $^{112,114,116}$Pd, as was similarly interpreted for $^{108}$Ru[24].

Based on the calculations in Refs. [17, 33] the triaxial minimum has an energy gain of 0.67 MeV in $^{108}$Ru and 0.32 MeV in $^{110}$Pd to indicate less pronounced triaxiality in the Pd isotopes. The fits by the standard IBM1 model and the rigid-triaxial version IBM1-V3 suggested $\gamma$ softness in $SU(6)$ $^{108}$Ru, and rigid triaxial deformations in $^{110,112}$Ru[76]. The less pronounced triaxiality in Pd may have disturbed the chirality in these nuclei, like the case of $^{108}$Ru where its $\gamma$-softness disturbed the chirality. The studies of chirality in Pd and Ru isotopes revealed an evolution from disturbed chirality in $^{112,114,116}$Pd with large but less pronounced triaxiality to chiral $^{110,112}$Ru with maximal triaxiality, like the evolution from $\gamma$ soft $^{108}$Ru to the chiral $^{110,112}$Ru[24].

The investigations of wobbling motions and chirality in Ru and Pd isotopes have thus implied that the maximal triaxial deformation is reached in $^{112}$Ru, and a less pronounced triaxial deformation reached and centered in $^{114}$Pd, which is four neutrons more than the calculations[17]. The studies of evolutions of wobbling motions and chirality in the Ru and Pd isotopic chains, respectively, have thus revealed a triaxial shape evolutions with changing neutron numbers. It is worth mentioning that although $^{108}$Ru is representative of a $\gamma$-soft nucleus, the triaxial minima become stabilized at a high rotational frequency $\hbar\omega\sim0.6$ MeV according to the TRS calculations in Ref. [1].

### 3.1.3 TRS calculations reproducing the systematics of band-crossings in Pd isotopes, describing the $\gamma$ driving of the $(\nu h_{11/2})^2$ and $(\pi g_{9/2})^2$ crossings to explain the wobbling motion in $^{114}$Pd, and revealing the long-sought shape evolutions and coexistence in neutron-rich Pd isotopes

The extended level schemes of the Pd isotopes (see, for example, the level scheme in Fig. 3) provided systematic data for the multiple band-crossings in Pd[30], namely the observations and/or absence of the first/second crossings and the related crossing fre-

quencies in the even-N and odd-N Pd isotopes, as can be seen in Fig. 9. The reproductions of the experimental band crossings by the TRS calculations shed light upon the long-sought shape evolutions and coexistence in the Pd isotopes, and the reproductions for $^{114}$Pd revealed large and stable triaxial deformations over a wide rotational frequency range which explained the onset of wobbling motion in $^{114}$Pd.

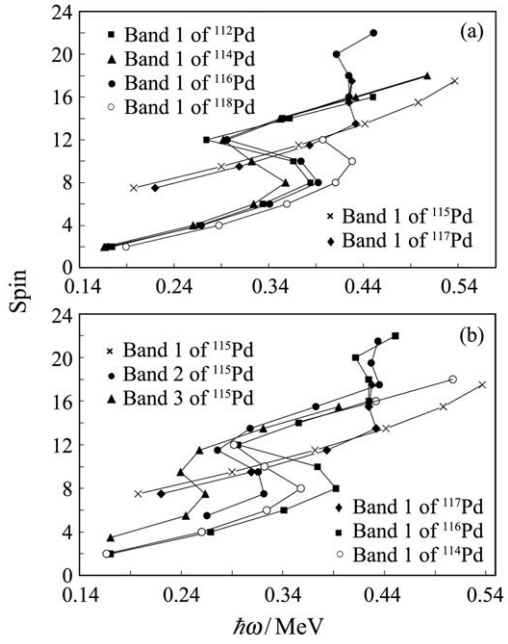


Fig. 9　Intriguing band-crossings observed in even-N (a) and in odd-N (b) Pd isotopes[30]. For comparison, bands in odd-N Pd isotopes and some in even-N Pd isotopes are also shown in (a) and (b), respectively.

The TRS calculations predicted pronounced driving effects of the $(\nu h_{11/2})^2$ and $(\pi g_{9/2})^2$ alignments. For $^{114,116,118}$Pd the calculated $(\nu h_{11/2})^2$ alignments were found to correlate with rapid up-rising $\gamma$ and $(\pi g_{9/2})^2$ alignments to correlate with dramatic decrease of $\gamma$ towards nearly oblate shape or more negative $\gamma$ (see Figs. 10 ∼ 13), the later supporting the prediction for the occurrence of oblate shape at high spins for isotopes with $Z \geqslant 41$, $N \geqslant 70$[5].

With good agreement between the experimental data and TRS calculations, the first band crossings observed in the even-N Pd isotopes was interpreted as $(\nu h_{11/2})^2$ alignments with up-rising $\gamma$ driving (Figs. 9 ∼ 11 and 13), which were not seen in band 1 of the odd-N isotopes due to the blocking from the $h_{11/2}$ odd-neutron. The second band crossing observed in $^{116}$Pd with the similar crossing frequencies as that in band 1 of $^{117}$Pd and that in the excited band 2 ($\nu g_{7/2}$ band) of $^{115}$Pd, and the missing (actually delayed, see below) second crossing in $^{114}$Pd are all interpreted as $(\pi g_{9/2})^2$ alignments with dramatic down-sloping $\gamma$ driving (Figs. 9 ∼ 13), showing different shape evolutions with increasing rotational frequency in neighboring Pd isotopes. The second crossing in $^{114}$Pd was predicted to occur at a rotational frequency around 0.1 MeV higher than that of $^{116}$Pd (see Figs. 10, 11 and 13), so the missing second crossing in $^{114}$Pd was most likely delayed to a higher frequency which was beyond the reach of the present experiment.

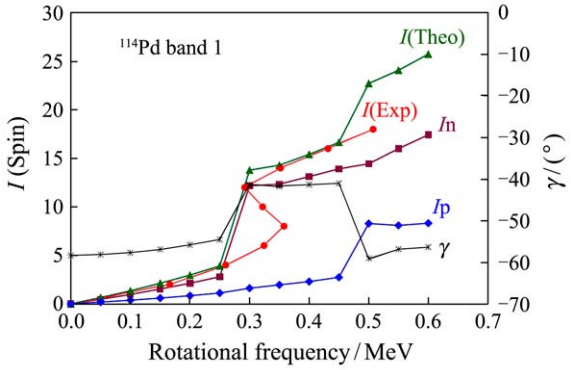


Fig. 10　(color online) TRS calculations for band 1 of $^{114}$Pd. $I$p and $I$n represent the angular momentum contributed by protons and neutrons, respectively. $I$(Theo) indicates the component along the cranking axis of the theoretical angular momentum, and $I$(Exp) represents the experimental angular momentum. The $\gamma$ values corresponding to energy minima calculated for $^{114}$Pd are also indicated in the figure. It is found that the first band crossing caused by $(\nu h_{11/2})^2$ alignment correlates to a rapid uprising $\gamma$, and the second band crossing caused by $(\pi g_{9/2})^2$ alignments correlates to a dramatic down-sloping $\gamma$ approaching a nearly oblate shape $\gamma \sim -60°$. It is the driving effects of both $(\nu h_{11/2})^2$ and $(\pi g_{9/2})^2$ alignments and the softness towards triaxiality that created a large and stable triaxial oblate deformation $\gamma \sim -41°$ over a wide rotational frequency range from ∼ 0.3 to 0.46 MeV, which explains the onset of wobbling motion and the good energy degeneracy of the doublet bands of $^{114}$Pd.

In Fig. 10 one can see that for the ground state and the states with rotational frequencies lower than ∼ 0.25 MeV $^{114}$Pd have $\gamma \sim -60°$, that is an oblate shape. One also sees $\gamma \sim -41°$ over the rotational frequency range from ∼ 0.3 MeV to as high as ∼ 0.46 MeV in the nucleus (Figs. 10 and 13), which is a large and stable triaxial deformation based on oblate shape, although the triaxiality is less pronounced than the maximal value in Ru. It is the large triaxial oblate deformations of $\gamma \sim -41°$ stabilized over a wide rotational frequency range that are responsible for the onset of wobbling motions [see Fig. 6(b)] and the very good energy degeneracy of the doublet bands in $^{114}$Pd (see Fig. 7). Keeping in mind the uprising $\gamma$ driving of

the $(\nu h_{11/2})^2$ alignments (first crossing) and the down sloping $\gamma$ driving of the $(\pi g_{9/2})^2$ alignments (second crossing) (see Fig. 10), one finds that in $^{114}$Pd it is the first $(\nu h_{11/2})^2$ crossing and the second $(\pi g_{9/2})^2$ crossing (delayed) and the nuclear softness towards large triaxiality that drive the nucleus to and stabilize the large triaxial oblate shape over such a wide frequency range. The delayed shape change from large triaxial oblate to nearly oblate manifested itself as the delayed second band crossing.

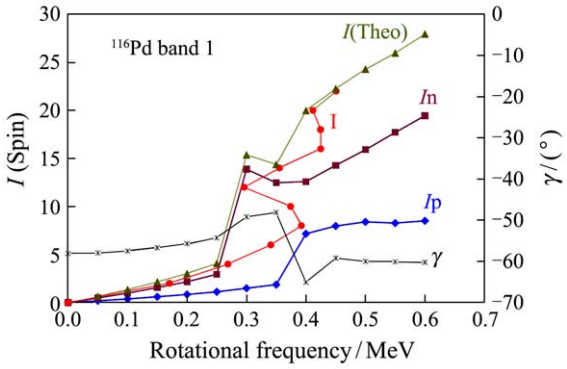


Fig. 11 (color online) The same as Fig. 10 but for band 1 of $^{116}$Pd. The TRS reproductions for the first crossing and second crossing are not as good as those for $^{114}$Pd, but reasonable agreement between the theoretical and experimental crossing frequencies is achieved. Much smaller rising of $\gamma$ is seen at the first crossing and the down-sloping $\gamma$ driving caused by the second crossing takes place much earlier than in $^{114}$Pd, most probably due to the tendency towards nearly oblate shapes, so that considerably smaller and less stable triaxiality is created in the frequency region, which explains the almost missing wobbling motion in this nucleus [see Fig. 6(c)]. See text.

Fig. 11 shows the TRS calculations against the data of $^{116}$Pd. The up-rising of $\gamma$ caused by the driving of $(\nu h_{11/2})^2$ alignment (first band crossing) is found to be much less pronounced, and the second band crossing caused by $(\pi g_{9/2})^2$ alignment with down-sloping $\gamma$ driving comes earlier than $^{114}$Pd, most probably due to the nuclear softness with a tendency towards nearly oblate shape, so that there is not a large and stable triaxial oblate shape maintained in $^{116}$Pd, but, instead, the overall nearly oblate shape is seen over a wide frequency range in $^{116}$Pd ($N = 70$). The above mentioned observations and interpretations have provided reasonable explanations for the almost disappearance of wobbling motions in $^{116}$Pd. The overall tendency that the near oblate shapes in $^{116}$Pd ($N = 70$) persist from zero to high frequency range (see Fig. 11) supports again the prediction in Ref. [5] that for $N \geqslant 70$ pronounced oblate shapes remain quite stable from ground state to high spin states. Such a stability of the oblate shapes is due to the simultaneous upper-shell neutron and proton Fermi surfaces, reinforced by the rotational alignment behavior. The observations of the dominance of oblate shapes in these heavy Pd isotopes are interesting since the collective rotations of the oblate structure are usually not favored energetically due to lower moments of inertia in comparison with those of prolate shapes.

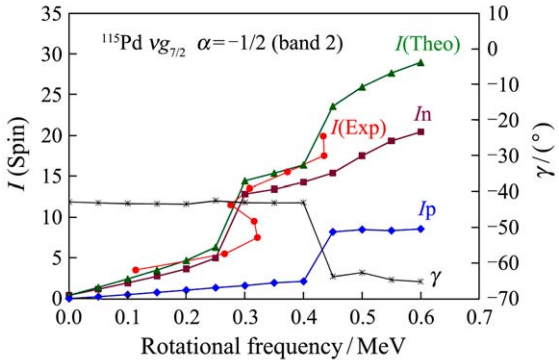


Fig. 12 (color online) The same as Fig. 10 but for the band 2, a $\nu g_{7/2}$, $\alpha = -1/2$ band of $^{115}$Pd. Very stable triaxial oblate shapes $\gamma \sim -41°$ remain over a wide rotational frequency region from zero to $\sim 0.40$ MeV. The first and second band crossings were well reproduced by the TRS calculations. However, no change of $\gamma$ is seen at the first crossing, showing the comparatively stable triaxial oblate shapes, which are maintained up to a high rotational frequency $\sim 0.40$ MeV until the second crossing caused by the $(\pi g_{9/2})^2$ alignment with strong down-sloping $\gamma$ driving pushes the nucleus to nearly oblate shapes. See text.

The TRS calculations well fitting the challenging band crossings observed in $^{115}$Pd revealed shape coexistence in the nucleus. The absence of second band-crossing of band 1 ($\nu h_{11/2}$ band) in $^{115}$Pd, which was, however, observed in band 1 of $^{117}$Pd, and the observation of this second crossing in band 2 ($\nu g_{7/2}$ band, $\alpha = -1/2$) of $^{115}$Pd (see Fig. 9) imply a shape coexistence in $^{115}$Pd. Shown in Fig. 12 are the TRS calculations for the band 2 of $^{115}$Pd. Large triaxial oblate shapes with $\gamma \sim -41°$ are seen to be so stable that the first band crossing did not cause any change of $\gamma$, most likely due to the pronounced tendency towards the large triaxiality, which is a different softness in comparison with that in $^{116}$Pd (see Fig. 11). The second band crossing observed in this excited band taking place at the same rotational frequency as that of the band 1 of $^{116}$Pd and $^{117}$Pd exhibits strong down-sloping $\gamma$ driving caused by the $(\pi g_{9/2})^2$ alignments, which finally drive the nucleus to nearly oblate shapes. In contrast to the stable triaxial oblate shapes in band

2, the band 1 has much less negative $\gamma$ or near triaxial prolate shapes due to the odd-$\nu h_{11/2}$ neutron.

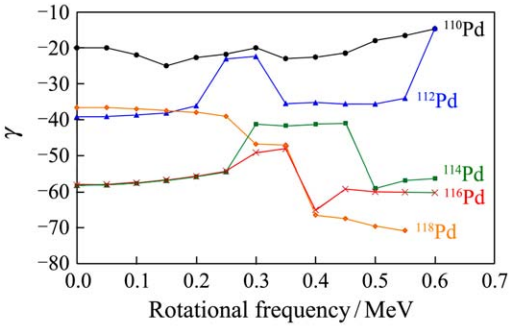


Fig. 13 (color online) $\gamma$ values corresponding to energy minima calculated for $^{110\text{-}118}$Pd by the TRS model[30]. In $^{114}$Pd the large triaxial oblate shapes $\gamma \approx -41^\circ$ stabilized over $\sim$ 0.30 to 0.46 MeV explained the triaxial wobbling motion [see Fig. 6(b)], the very good energy degeneracy over wide spin range in the doublet bands (see Fig. 7), and the delayed second crossing in this isotope. The ground states and those lower than ∼0.2 MeV of $^{114,116}$Pd have $\gamma \approx -60^\circ$ for an oblate shape while $^{110}$Pd has $\gamma \approx -20^\circ$, a triaxial prolate shape, and $^{112,118}$Pd have $\gamma \approx -40^\circ$, triaxial oblate shapes at low $\hbar\omega$ but shape fluctuations at higher frequencies, showing a more complete but complex picture of shape evolutions than earlier predictions. See the following text.

Well reproducing the intriguing band-crossings observed in $^{112,114\text{–}118}$Pd, the systematic TRS calculations have given an answer to the long-sought shape evolution for their ground states and levels with rotational frequency lower than $\sim$ 0.2 MeV, that is, with increasing neutron number, $^{110\text{–}118}$Pd undergo an overall shape evolution from triaxial prolate in $^{110}$Pd via triaxial oblate in $^{112}$Pd to nearly oblate in $^{114,116}$Pd, and then back to less negative $\gamma$ value in $^{118}$Pd (see Fig. 13), with shape coexistence deduced in $^{115}$Pd, which is a more complete but complex picture than the previous predictions. Furthermore, shape evolutions with increasing rotational frequency in Pd isotopes are also revealed by reproducing the data by TRS calculations as can be seen in Figs. 9 ∼ 13, and as discussed in some details above.

### 3.1.4 Quasi-particle couplings, quasi-rotations, onset of collectivity and triaxiality in Cd ($Z = 48$) isotopes

A new partial level scheme of $^{120}$Cd is given in Fig. 14 which includes 20 new transitions and two new bands, serving as an example of those of $^{117\text{–}120,122}$Cd[43].

Based on the level schemes of the even-N Cd isotopes (see that of $^{120}$Cd in Fig. 14), the ratio of the

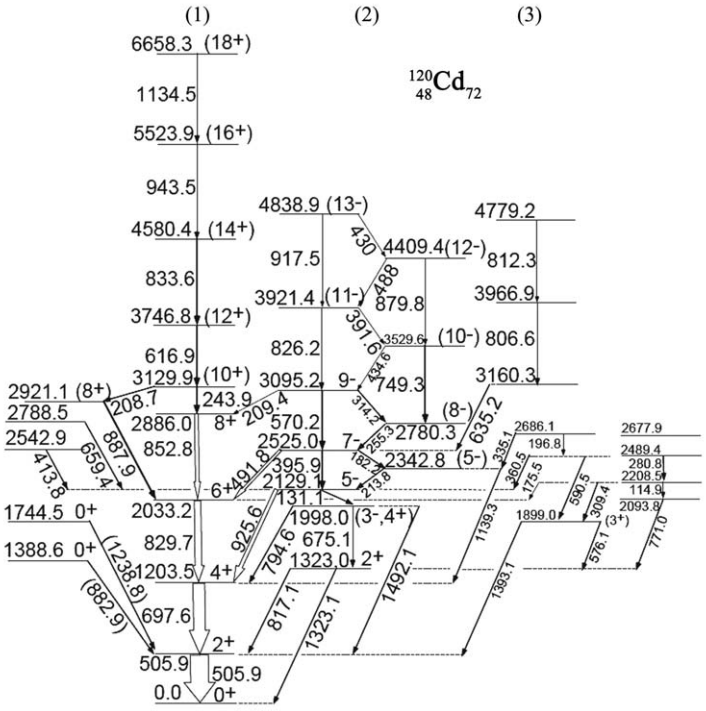


Fig. 14 New partial level scheme of $^{120}$Cd[43], an example of those of the Cd isotopes. Note the level pattern of band 1 characteristic of quasi-particle couplings and quasi-rotations (see text and Figs. 15 ∼ 16). The $5^-$ state was interpreted as quadrupole-octupole-coupled (QOC) state, which was, however, challenged by a study of a deuteron-induced reaction[42].

excitation of the first $4^+$ to that of the first $2^+$ level is found to be $\sim 2.38$, in contrast to 2.56 in Pd, 2.76 in Ru, and 3.0 in Mo isotopes, implying a decrease of collectivity while approaching the $Z = 50$ major shell closure. However, increasing quasi-collectivity with spins have been implied by analyzing the systematic excitations of the even-N and the neighboring odd-N Cd isotopes. Fig. 15 shows the comparison among the excitations of $2^+$, $4^+$, $6^+$, $8^+$, $10^+$ in $^{114-122}$Cd (solid symbols) with those above the $11/2^-$ state of $15/2^-$, $19/2^-$, $23/2^-$, $27/2^-$, $31/2^-$ in $^{113-121}$Cd (open symbols). Below the $6^+$ (and $23/2^-$) levels, the transition energies of $^{113-121}$Cd are quite similar to those of their neighboring $^{114-122}$Cd isotopes, showing stretch-coupling of the odd-neutron's 11/2 spin to the band members of the even-even neighbors. However, increasing deviations are seen with increasing spin, which may imply weakened coupling and increasing role of the quasi-rotational degree of freedom.

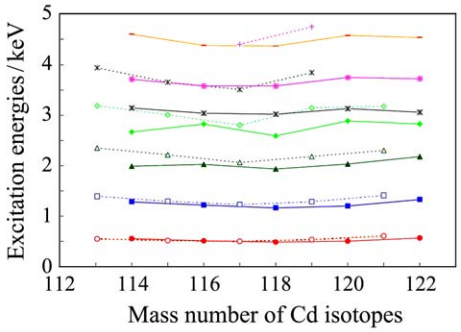


Fig. 15 (color online) The weakening of the stretch-coupling with increasing spins seen in $^{113-122}$Cd. Quasi-collectivity may increase with increasing spins in the Cd isotopes. See text. Onset of considerable collectivity in the vicinity of closed shells was also implied by recent studies of Coulomb excitations of the secondary beams of $^{122,124,126}$Cd at REX-ISOLDE at CERN[46]. See text.

The SCTAC model for nearly spherical nuclei using slightly deformed shape parameters ($\beta_2 = 0.1 \sim 0.2$, $\gamma = -10°$ to $-15°$)[44–45] well reproduced the moments of inertia plotted against rotational frequency of the ground bands of $^{104-114}$Cd. The model-independent plots of experimental spin ~ rotational frequency of even-N $^{116,118,120,122}$Cd (Fig. 16) exhibit the same variations as seen in $^{104-114}$Cd, showing evidence for slightly deformed shapes with small to medium triaxial deformations. Small to medium triaxial deformations were also suggested for odd-N $^{113,115,117}$Cd by triaxial-rotor-plus-particle model reproductions of $B$(E2, $7/2^- \rightarrow 11/2^-$) values in the odd-N Cd isotopes[43]. The small to medium triaxial deformations suggested in Cd isotopes are most likely soft since only a behavior of quasi-rotation was seen in the bands observed.

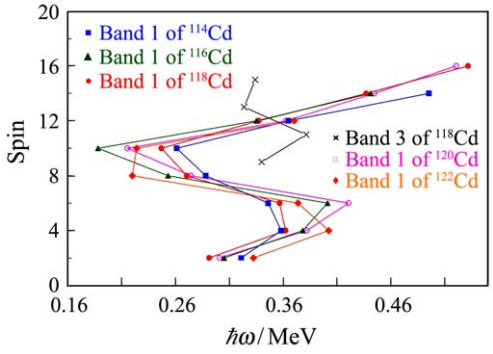


Fig. 16 (color online) The sharp band-crossings in quasi-rotations of even-N Cd isotopes[43] in a model-independent plot showing quasi-collectivity in these nuclei with only two proton holes in the $Z = 50$ major shell. The crossings were reasonably reproduced by TRS calculations. See text.

Systematic TRS calculations were also carried out for the Cd isotopes, reproducing the sharp band-crossings in even-N Cd isotopes as caused by the quasi-rotational alignment of $(\nu h_{11/2})^2$ at $\sim 0.4$ MeV, and for $(\pi p_{1/2})^2$ at $\sim 0.65$ MeV[43]. The former are ~0.05 MeV larger than the experiment, but still in fairly good agreement with the experimental crossing frequencies (Fig. 16), which may imply quasi-collectivity of the Cd isotopes, although the applicability of the TRS model for such nuclei very close to the $Z = 50$ shell closure may be questionable.

Onset of collectivity in Cd isotopes, in the vicinity of both the $Z = 50$ and $N = 82$ shell closures, was very recently proposed in a detailed and important investigation by means of Coulomb excitations[46]. The Coulomb excitations of $^{122,124,126}$Cd ($Z = 48$ and $N = 74$, 76, 78) produced in induced fission of $^{238}$U were measured at the radioactive ion-beam facility REX-ISOLDE at CERN, where a 1.4 GeV proton beam was provided by the PS-Booster and hit a neutron converter to enhance the productions of Cd isotopes. The Cd isotopes were $Z/A$ separated and post-accelerated to deliver the secondary Cd beams, which then bombarded $^{108}$Pd, $^{104}$Pd and $^{64}$Zn target, respectively, with optimal Coulomb excitation cross-sections for the Cd isotopes. The reduced transition probabilities $B$(E2; $0^+_{\rm g.s.} \rightarrow 2^+_1$) for the excitations of the $2^+_1$ states were determined to be 0.41(20) $e^2$b$^2$, 0.35(19) $e^2$b$^2$, and 0.27(6) $e^2$b$^2$ for $^{122}$Cd, $^{124}$Cd and $^{126}$Cd, respectively. The comparison with theories indicated that a beyond mean field (BMF) theory well described the experimental $B$(E2) values, revealing moderate collectivities, unusual for nuclei with so few valence holes in the closed shells. The decreasing $B$(E2; $0^+_{\rm g.s.} \rightarrow 2^+_1$) with increasing neutron number

also showed no evidence for the possible quenching of the $N = 82$ closed shell, which is of current interest. The quadrupole moments of the $2_1^+$ states determined favored a spherical shape for the Cd isotopes, but, however, the measurements of the quadrupole moments have large uncertainties[46].

### 3.2 Shape changes and coexistence with regard to triaxiality in Zr, Nb, Mo and Tc isotopes with $Z$ below Ru

The Sr, Y and Zr isotopes are considered to be axially symmetric with strong quadrupole deformations (*e.g.* Ref. [1]). The $\gamma$ degree of freedom was first proposed in Mo-Tc-Ru region. The crossing frequencies of the $(\nu h_{11/2})^2$ alignments in the even-N Mo isotopes was found to be lower than those of the even-N $^{100-104}$Zr, which was accounted for by the triaxial degree of freedom in the Mo and axially symmetric shapes in Zr isotopes[47]. The different signature splittings of the $\nu h_{11/2}$ band in the odd-N Mo and Zr isotopes were also attributed to the triaxial deformations in Mo isotopes. Triaxial ground-state minima around $\gamma \sim 20°$ were calculated for $^{104,106}$Mo[1]. Chiral symmetry breaking was proposed in $^{106}$Mo[7] and $^{108}$Mo[54]. However, in a very recent work preliminary information concerning triaxiality in heavier Zr isotopes $^{104-106}$Zr was reported[48]. The newly observed bands of $^{104-106}$Zr were reproduced by an improved IBM model calculations which includes triaxial degree of freedom. Mean-field calculations[77] yielded a prolate minimum and an oblate minimum which are separated by a shallow ridge in the triaxial plane. As mentioned above, pronounced shape transition from prolate to oblate in Zr was predicted for $N \geqslant 70$[5], but experimental data are now not experimentally available. For Tc isotopes, moderate quadrupole deformations $\varepsilon_2 = 0.32$, and medium to large triaxiality increasing with neutron number from $\gamma \sim -22.5°$ to $-26°$ were deduced in Tc ($Z = 43$)(*e.g.* Ref. [10]). Chiral doublet bands were reported in $^{100}$Tc[78]. Moderate to large quadrupole deformations $\varepsilon_2 \sim 0.25$ to 0.37 and small to medium triaxiality of $\gamma \sim 5°$ to 19° were proposed in the previously studied Nb ($Z = 41$) isotopes by RTRP model[4].

Very recently, the detailed study of heavier odd-odd Nb isotopes $^{104,106}$Nb[59] and the re-studies of $^{101-103,105}$Nb[60–61, 79] provided significant information to reveal their transitional behavior with regard to soft triaxial deformations. PES and PSM calculations well reproduced the experimental data, showing a picture of $\gamma$ shape evolution with increasing excitations/spins as well as with changing neutron number.

#### 3.2.1 Level schemes of the very neutron-rich odd-odd Nb isotopes

Weakly-populated bands were identified and extended in $^{106,104}$Nb[57, 59]. Figs. 17 and 18 shows the

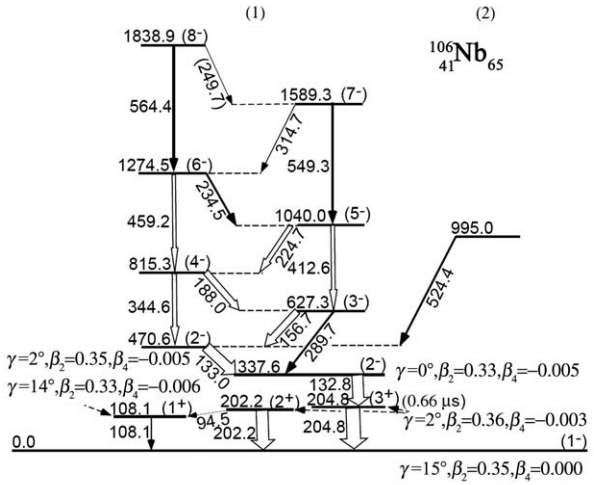


Fig. 17 Level scheme of $^{106}$Nb proposed for the first time[59]. Spin/parity and shapes that were deduced by PES and PSM calculations are shown. Configuration assignments can be found in Table 2. The model calculations well reproduced the isomeric decay of the 204.8 keV level, and suggested shape transitions from medium triaxial deformation at ground state to near axial symmetric shapes for excited levels and the band-head.

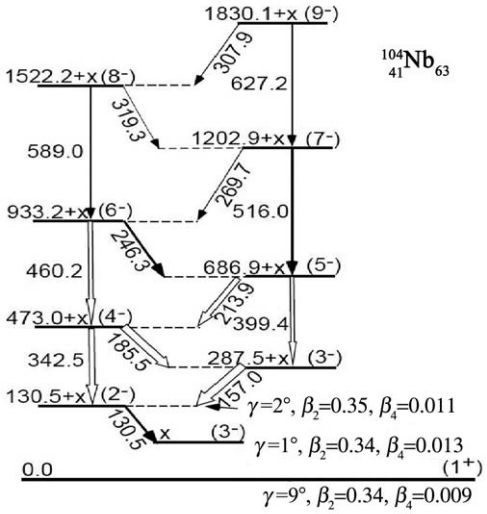


Fig. 18 Extended level scheme of $^{104}$Nb[57, 59]. Spin/parity and shapes deduced by PES and PSM model calculations are shown. Configuration assignments are indicated in Table 2. One can see similar level pattern but different decay out pattern in comparison to those of $^{106}$Nb, both of which are well reproduced by the model calculations. One can see similar shape transitions with regard to triaxiality as seen in $^{106}$Nb. However, a considerably smaller triaxial deformation in $^{104}$Nb than that in $^{106}$Nb was deduced.

level scheme of $^{106}$Nb observed for the first time[59] and that of $^{104}$Nb[57, 59] extended, respectively. Analogous band structure and different decay-out patterns are well reproduced by PES and PSM calculations for the two isotopes as seen in the figures.

### 3.2.2 Triaxial shape evolutions in Nb isotopes deduced by comparison of experimental bands for odd-odd $^{104,106}$Nb with PES and PSM model calculations

PES calculations were made to reproduce the ground states, low-lying states and band-heads of $^{106,104}$Nb[59]. Configurations, spin/parities and shapes assignments were deduced for the levels. Medium triaxiality $\gamma = 15°$ and 9° were deduced for the ground levels of $^{106}$Nb and $^{104}$Nb, respectively. Large quadrupole deformations with nearly axially symmetric shapes $\gamma = 0°$ to 2° were deduced for the excited levels of the two isotopes, except for the first excited 108.1 keV level in $^{106}$Nb (see Table 2 and Fig. 17). Medium triaxial deformations in their ground states and evolutions to near axially-symmetric shapes with increasing spins are proposed in $^{104,106}$Nb.

Table 2 PES and PSM calculations for the ground levels, low-lying levels and band-heads of $^{106,104}$Nb[59]. Large $\beta_2$ and evolutions of triaxial deformation were deduced.

| Nucleus | $E_{\rm EXP}$ | $E_{\rm PES}$ | $E_{\rm PSM}$ | Spin/parity | Configuration | Shape (PES) | Shape (PSM) |
|---|---|---|---|---|---|---|---|
| $^{106}$Nb | 0 | 0 | 0 | $(1^-)$ | $\pi 3/2^-[301]\times\nu 5/2^+[413]$ | $\beta_2=0.35,\ \gamma=15°,\ \beta_4=0.000$ | $\beta_2=0.417,\ \beta_4=0.079$ |
| | 0.1081 | 0.171 | | $(1^+)$ | $\pi 3/2^-[301]\times\nu 5/2^+[532]$ | $\beta_2=0.33,\ \gamma=14°,\ \beta_4=0.006$ | |
| | 0.2022 | 0.203 | | $(2^+)$ | $\pi 1/2^-[431]\times\nu 5/2^+[413]$ | $\beta_2=0.36,\ \gamma=2°,\ \beta_4=-0.003$ | |
| | 0.2048 | 0.203 | | $(3^+)$ | $\pi 1/2^-[431]\times\nu 5/2^+[413]$ | $\beta_2=0.36,\ \gamma=2°,\ \beta_4=-0.003$ | |
| | 0.3376 | 0.238 | | $(2^-)$ | $\pi 3/2^-[301]\times\nu 1/2^+[411]$ | $\beta_2=0.33,\ \gamma=0°,\ \beta_4=-0.005$ | |
| | 0.4706 | 0.506 | 0.660 | $(2^-)$ | $\pi 1/2^+[431]\times\nu 5/2^-[532]$ | $\beta_2=0.35,\ \gamma=2°,\ \beta_4=-0.005$ | $\beta_2=0.417,\ \beta_4=0.079$ |
| $^{104}$Nb | 0 | 0 | 0 | $(1^+)$ | $\pi 3/2^-[301]\times\nu 5/2^-[413]$ | $\beta_2=0.34,\ \gamma=9°,\ \beta_4=0.009$ | $\beta_2=0.402,\ \beta_4=0.035$ |
| | x | 0.111 | | $(3^-)$ | $\pi 3/2^-[301]\times\nu 3/2^+[411]$ | $\beta_2=0.34,\ \gamma=1°,\ \beta_4=0.013$ | |
| | 0.1305+x | 0.114 | 0.444 | $(2^-)$ | $\pi 1/2^+[431]\times\nu 5/2^-[532]$ | $\beta_2=0.35,\ \gamma=2°,\ \beta_4=-0.011$ | $\beta_2=0.402,\ \beta_4=0.035$ |

A $K^\pi = 2^-$, $\pi 1/2^+[431]$ (intruder) $\times\nu 5/2^-[532]$ configuration was assigned to the band-heads of $^{106,104}$Nb. $3^+$, $\pi 1/2^+[431]\times\nu 5/2^+[413]$ was assigned to the 204.8 keV isomer in $^{106}$Nb, and the M2 character of the 204.8 keV transition explained the 204.8 keV isomeric decay from the 0.66 μs isomer (Fig. 17). However, in $^{104}$Nb the $3^+$ state is bypassed by the very low excitation of the band-head (see Table 2 and Fig. 18). The proton intruder $\pi 1/2^+[431]$ plays an important role in the shape evolution with regard to triaxiality.

The PSM calculations were performed to reproduce the level excitations $E_{\rm exc}$ and moments of inertia $J^{(1)}$ of the bands of $^{104,106}$Nb[59]. The PSM calculations of $E_{\rm exc}$ and $J^{(1)}$ on $2^-$, and $3^-$, $\pi 1/2^+[431]\times\nu 5/2^-[532]$ configurations of $^{106}$Nb are shown in Fig. 18 and 19, respectively. One can see that the calculations based on $K^\pi = 2^-$, $\pi 1/2^+[431]\times\nu 5/2^-[532]$, which was also deduced by the PES calculations, well described the band of $^{106}$Nb. All the PSM calculations with spin/parity/configuration other than $K^\pi = 2^-$, $\pi 1/2^+[431]\times\nu 5/2^-[532]$ yielded large discrepancies in comparison to the experimental data.

Agreement between the PES and PSM calculations achieved for these levels is impressive (see Table 2). The nearly axially symmetric shapes calculated for the band-heads justify the use of PSM calculations for the bands of these odd-odd nuclei. Since the intruder orbital $\pi 1/2^+[431]$ is involved in the band-heads, the cranking TRS would not be convergent, and not applicable for the bands of both isotopes.

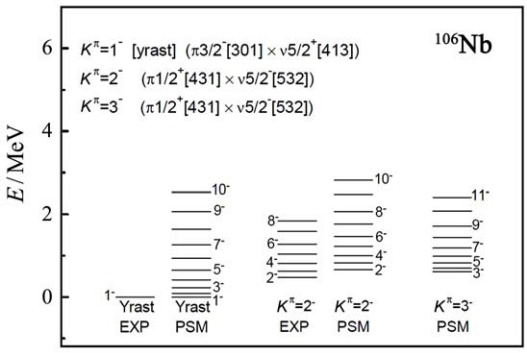


Fig. 19 PSM calculations for $E_{\rm exc}$ based on $2^-$, and $3^-$, $\pi 1/2^+[431]\times\nu 5/2^-[532]$ for $^{106}$Nb. Calculations based on $2^-$, $\pi 1/2^+[431]\times\nu 5/2^-[532]$ well reproduced the level excitations. A near axially-symmetric shape with large quadrupole deformation $\gamma = 2°$, $\beta_2 = 0.35$, $\beta_4 = -0.005$ (see Table 2) was deduced for the band of $^{106}$Nb.

Successful reproductions for $E_{\rm exc}$ and $J^{(1)}$ of the analogous band in $^{104}$Nb by PSM calculations also based on $K^\pi = 2^-$, $\pi 1/2^+[431]\times\nu 5/2^-[532]$ were achieved as well, which are very similar to those shown in Fig. 19 and Fig. 20, respectively. A near axilly-symmetric shape with large quadrupole deformation $\gamma = 2°$, $\beta_2 = 0.35$, $\beta_4 = 0.011$ was also deduced for the band of $^{104}$Nb[59].

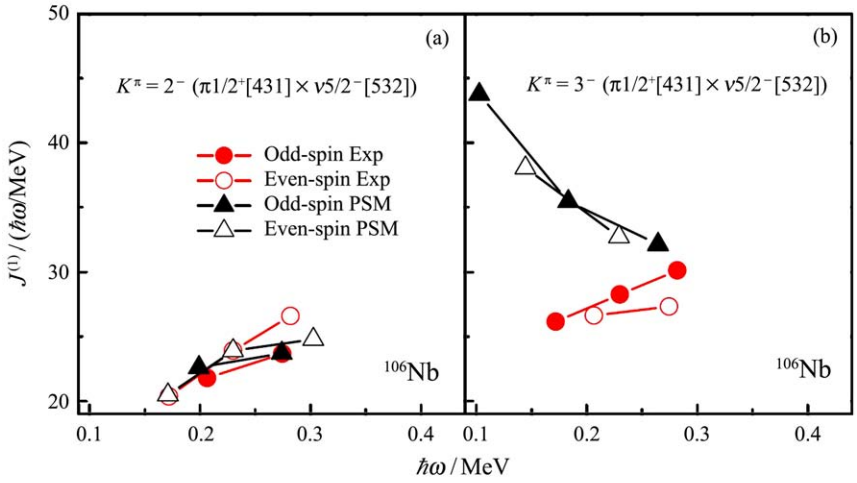


Fig. 20　PSM calculations for the moments of inertia $J^{(1)}$ based on $2^-$ (a), $3^-$ (b), and $\pi 1/2^+[431] \times \nu 5/2^-[532]$ for $^{106}$Nb. Again, calculations based on $2^-$, $\pi 1/2^+[431] \times \nu 5/2^-[532]$ well reproduced the $J^{(1)}$.

### 3.2.3 The recent studies of $^{101-103,105}$Nb, the identifications of one-phonon and two-phonon $\gamma$ vibrational bands in $^{103,105}$Nb, the soft triaxial shape evolutions in the Nb isotopic chain, and shape coexistence in $^{101,103}$Nb

Very recently even-N Nb isotopes $^{103,105}$Nb were re-studied[60–61]. Three new bands were observed in the isotopes based on the fission data mentioned above. PES and TPSM (triaxial projected shell model) calculations were performed to reproduce the level structure. One-phonon and two-phonon $\gamma$ vibrational bands were proposed in the isotopes, implying the importance of the triaxial degree of freedom in the Nb isotopes. The TRS calculations for $^{105}$Nb yielded a minimum at $\gamma = 12.3°, \beta_2 = 0.339$ and $\beta_4 = 0.007$ for $\hbar\omega = 0.0$ MeV, a $\gamma$ value between those of the ground states of $^{106}$Nb and $^{104}$Nb.

The TRS calculations for the $\pi 5/2^+[422]$ bands of $^{101,103}$Nb were recently carried out. For $\hbar\omega = 0.0$ MeV in the contour plots, a minimum at $\gamma = 1.2°$, $\beta_2 = 0.378$, $\beta_4 = 0.019$ for $^{103}$Nb, and another at $\gamma = 0.57°$, $\beta_2 = 0.298, \beta_4 = 0.034$ for $^{101}$Nb was found, respectively, indicating near axially-symmetric shapes with large quadrupole deformations in the two isotopes. Shown in Figs. 21 and 22 are the TRS calculations for the $\alpha = +1/2$ and $\alpha = -1/2$ signature of the $\pi 5/2^+[422]$ band of $^{103}$Nb, respectively. The minima in the contour plots are all shallow, implying the soft shapes of the isotopes. It can be seen in Fig. 21 that for the $\alpha = +1/2$ signature of the $\pi 5/2^+[422]$ band of $^{103}$Nb, with increasing rotational frequency the $\gamma$ value corresponding to the minimum changes from $\gamma = 1.2°$ at $\hbar\omega = 0.0$ MeV, a near axially-symmetric shape, through a very unstable region to a minimum at $\gamma = 14.5°$ for $\hbar\omega = 0.3$ MeV, a medium soft triaxial deformation.

However, as shown in Fig. 22 for the $\alpha = -1/2$ signature, large $\beta_2$ and near axially-symmetric shapes remain over a wide rotational frequency region up to $\hbar\omega = 0.3$ MeV, with medium $\gamma$ deformations appearing at higher rotational frequencies in comparison with the observation in Fig. 21 (the contour plots with $\omega$ larger than 0.3 MeV being not indicated in the figure). The Figs. 21 and 22 thus show a picture of shape evolution with increasing $\hbar\omega$, and a triaxial shape coexistence in the two signatures of the $\pi 5/2^+[422]$ band of $^{103}$Nb. Similar results were obtained for the $\pi 5/2^+[422]$ band of $^{101}$Nb.

The $K^\pi = 2^-$, $\pi 1/2^+[431] \times \nu 5/2^-[532]$ were also assigned to the band-head of the analogous $^{102}$Nb by recent PES calculations, and near axially-symmetric shapes were deduced for both the ground state and the band-head of $^{102}$Nb. The PSM calculations based on $K^\pi = 2^-, \pi 1/2^+[431] \times \nu 5/2^-[532]$ have recently been carried out and well reproduced the analogous band in $^{102}$Nb[79]. Again, agreement between the PES and PSM calculations was achieved for $^{102}$Nb.

Since a shape evolution from spherical to strong quadrupole deformations with increasing neutron number in Nb isotopic chain was identified, and $N = 59$ ($^{100}$Nb) was found to be the onset point of strong quadrupole deformations[58], all the above- mentioned results concerning triaxial deformations in the Nb isotopic chain indicate an overall slight increase of soft triaxial deformations with increasing neutron number in $^{100-106}$Nb. Soft triaxial shape evolutions with increasing spins were also seen in the Nb isotopes.

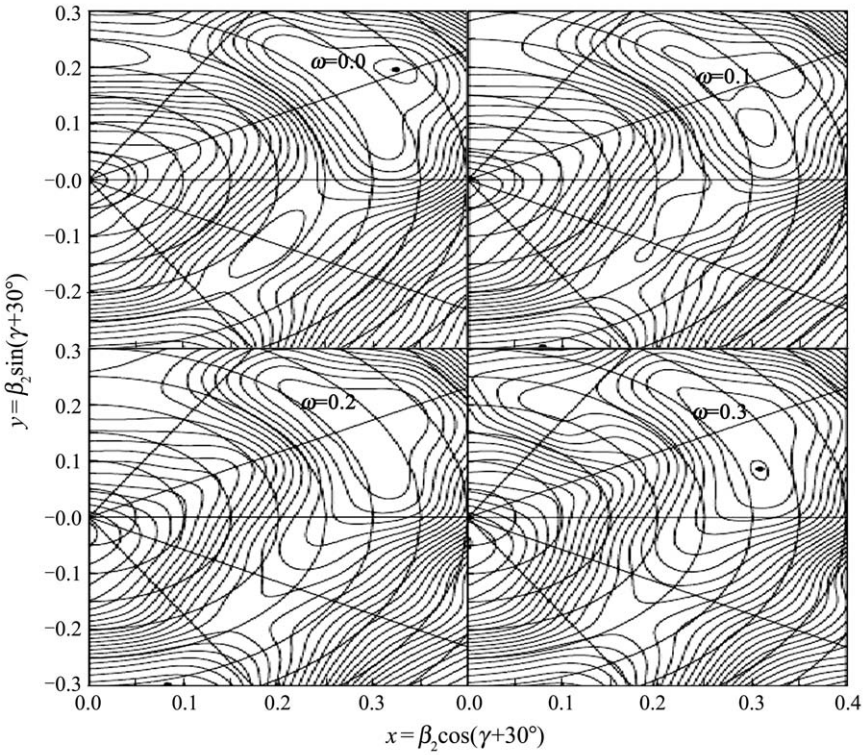


Fig. 21 Contour plot of the recent TRS calculations for the $\alpha = +1/2$ signature of the $\pi 5/2^+[422]$ band of $^{103}$Nb. Shallow minima are calculated. A soft triaxial shape evolution is seen with increasing rotational frequency. Continuous slight increase of γs is found at higher frequencies which are not shown here.

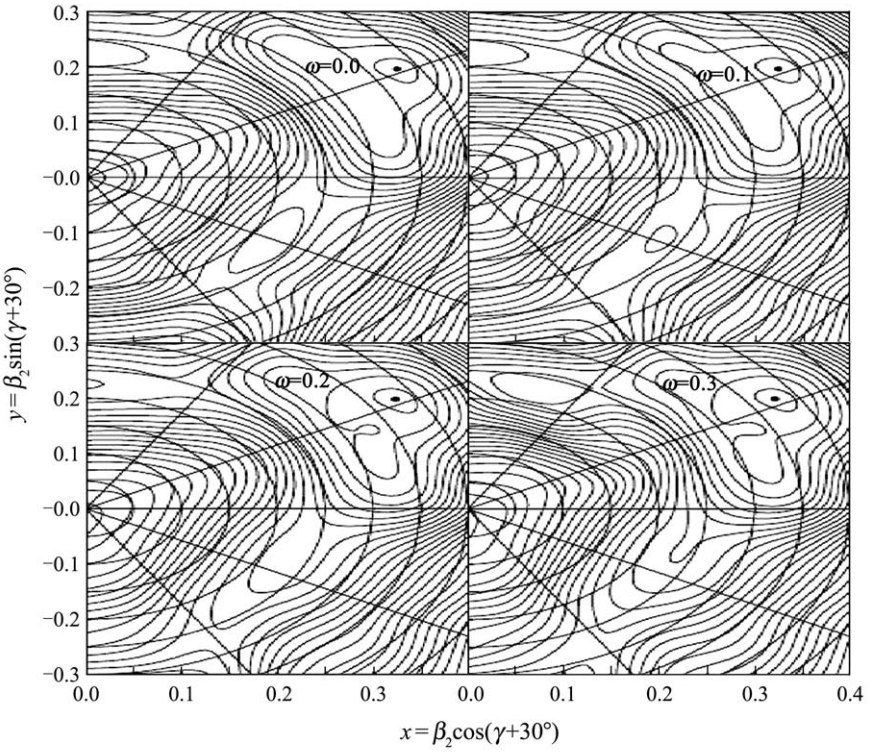


Fig. 22 Contour plot of the recent TRS calculations for the $\alpha = -1/2$ signature of the $\pi 5/2^+[422]$ band of $^{103}$Nb. In contrast to Fig. 21, a near axially-symmetric shape of large quadrupole deformation is seen to remain over a wide rotational frequency range. For $\hbar\omega > 0.3$ MeV, minima corresponding to medium γs are seen, which are not shown in the figure because of space constraint. See text for details.

## 4 Concluding remarks

Based on the systematic work on prompt fission $\gamma$ spectroscopy, and combined with previous achievements and some new progresses made by other methods, the nuclear shape transition and coexistence with regard to triaxiality were proposed to evolve with changing $Z$, $N$ and excitation/spins in the neutron-rich nuclei with $Z = 41$ through $Z = 48$. An overall gradual decreasing triaxial deformations with decreasing proton number was deduced in nuclei with $Z$ below Ru ($Z = 44$), and a decreasing triaxiality with increasing proton number in nuclei with $Z$ beyond Ru. The changing softness to triaxiality may have caused the emerging and developing triaxial degree of freedom in this nuclear region. $\gamma$ degree of freedom was found to be highly involved in the prolate-oblate transitions, and the new excitation modes built on triaxiality have opened a new frontier for the studies of nuclear structure.

By studying the evolution and onset of chiral doubling in Ru and Pd, maximal triaxial deformations in Ru isotopes and changing triaxiality in Ru-Pd isotopes were suggested. While chiral symmetry breaking was identified in triaxial $^{110,112}$Ru, disturbed chirality was proposed in the $N = 68$ isotone and nearby isotopes $^{112,114,116}$Pd, implying less pronounced triaxial deformations in the Pd isotopes. The evolutions and onset of wobbling motions with changing $Z$, $N$ and spins yielded additional evidence for the changing triaxial deformations. The deduced center of maximal triaxial deformations in $^{112}$Ru and that of less pronounced triaxial deformations in $^{114}$Pd are four neutrons heavier than the calculations[17]. The deviation between the theory and the current experimental studies is likely due to the shape evolution from the ground state to medium and high spin regions. Based on the TRS reproductions of intriguing band-crossings observed in the Pd isotopic chain, pronounced $\gamma$ drivings of the $(\nu h_{11/2})^2$ and $(\pi g_{9/2})^2$ crossings were suggested, the large triaxial deformations at a wide rotational frequency range and consequently onset of wobbling motions in $^{114}$Pd were explained, and an overall shape evolution in $^{110–118}$Pd was deduced to go from triaxial prolate via triaxial oblate to nearly oblate, and then back to less negative $\gamma$ value, with shape coexistence identified in $^{115}$Pd, which is a more complete but complex picture than the previous predictions. The TRS calculations well reproduced the band-crossings and thus described the triaxial shape evolutions with changing spins and excitations in Pd.

The long isotopic chain of Rh covered by chiral symmetry breaking support the near maximal triaixlity deduced by RTRP model for the Rh isotopes. Very rich structural phenomena, chiral breaking, magnetic rotation, and principal axis rotation, were reported in the soft Ag isotopes, and triaxial deformations may play an important role in the nuclear structure. For Cd isotopes with only few valence holes in the closed shells, evolution of quasi-collectivity with spins and neutron number, and small to medium but soft triaxial deformations were proposed. Combining the progresses based on prompt fission $\gamma$ spectroscopy and the studies of Coulomb excitations of secondary beams, important steps forward were made for the investigations of the onset of collectivity including soft triaxiality in the vicinity of the closed shells.

While Y and Zr isotopes were shown to be axially-symmetric, evidence for the emergence of the triaxial degree of freedom was found for heavier $^{104–106}$Zr, and oblate shapes were predicted for even heavier Zr isotopes with $N \geqslant 70$. An overall increase of triaxial deformations from axially-symmetric shapes to soft medium $\gamma$ with increasing neutron number were also deduced for the ground states in $^{100–106}$Nb. Soft triaxial shape evolutions and coexistence with changing spins in Nb isotopes were suggested as well. The TRS, PES and PSM calculations well reproduced the level structure of the odd-odd $^{104,106}$Nb isotopes to indicate shape evolutions from medium triaxial with large quadrupole deformations at ground states to near axial symmetric shapes at excited levels and the band-heads, showing an important role of the proton intruder orbital $\pi 1/2^+[431]$. Re-studies of the neighboring even-N Nb isotopes and the recent TRS calculations for $^{101–103}$Nb yielded additional information for the soft triaxial deformations in the Nb isotopes. The studies of chiral symmetry breaking, band-crossings, signature splitting and $\gamma$ vibrational bands in Mo and Tc isotopes in comparison with the band-crossing and signature splitting in light Zr isotopes provided valuable information for the triaxial shape evolutions in Ru-Tc-Mo-Zr isotopes.

The shape transitions from prolate through triaxial to oblate identified in Pd isotopes support the theoretical prediction that with increasing neutron number in the nuclei with $Z \geqslant 40$, nuclear shapes evolve from prolate through triaxial deformations to oblate, and the pronounced oblate shapes dominate at $N \geqslant 70$. The identifications of triaxial wobbling motions in the first and second wobbler, $N = 68$ isotone $^{112}$Ru and $^{114}$Pd, the evolutions of wobbling motions along the Ru and Pd isotopic chains, and the identifications of chiral doubling in $^{110,112}$Ru and the disturbed chirality in Pd isotopes, especially in $^{114}$Pd, strongly support the prediction. The interesting shape coexistence de-

duced in $^{115}$Pd with $N=69$, the even-odd neighbor of $^{114}$Pd, may very likely be identified also in the neighboring isotopic chain. Further attention seems needed to verify this prediction. The $N \geqslant 70$ region, including the isotopes which are currently beyond reach, is of special interest. More experimental and theoretical efforts are crucial for the studies of Cd isotopes in the vicinity of closed shells, where ambiguities remain in both studies of prompt fission $\gamma$ spectroscopy and Coulomb excitations.

Strong and rapid $\gamma$ drivings of the first and second crossing caused by $(\nu h_{11/2})^2$ and $(\pi g_{9/2})^2$ alignments, respectively, was found to play one of the key roles for the shape changes with regard to triaxiality at medium to high spins, most likely due to the pronounced softness towards triaxial deformations in this nuclear region.

**Acknowledgments** The work at Vanderbilt University, Lawrence Berkeley National Laboratory, University of Notre Dame, Oak Ridge National Laboratory, Lawrence Livermore National Laboratory, and Mississippi State University was supported by the U.S. DOE Grants and Contracts No. DE-FG-05-88ER40407, DE-AC02-05CH11231, DE-FG02-95ER40934, DE-AC05-00OR22725, DE-AC52-07NA27344, DE-FG02-95ER40939. The work at Tsinghua University was supported by the National Natural Science Foundation of China under Grants No. 11175095, 10975082, and the Special Program of Higher Education Science Foundation under Grant No. 2010000211007. The work at Peking University was supported by the National Natural Science Foundation of China under Grants No. 11235001 and No. 11320101004. The work at HUTC in Huzhou was supported by the NNSF of China under Grant Nos. 11305059, 11275063 and 11275068. The work at SJTU in Shanghai was supported by the NNSF of China under Grant Nos. 11135005, 11075103 and by the National Basic Research Program of China, Grant No. 2013CB834401. The work at JINR, Dubna, was supported by the Russian Foundation for Basic Research through Grant Nos. 11-02-12050 and 11-02-12066.

**References:**

[1] SKALSKI J, MIZUTORI S, NAZAREWICZ W. Nucl Phys A, 1997, **617**: 282.
[2] HAMILTON H. Prog in Particle and Nucl Phys, 1985, **15**: 107; Treatise on Heavy Ion Science, ed. D. ALLAN BROMLEY. Plenum, NY, 1989, **8**: 363.
[3] ZHU S J, LUO Y X, HAMILTON J H, *et al.* Inter Jour of Modern Phys E, 2009, **18**(8): 1717.
[4] LUO Y X, RASMUSSEN J O, STEFANESCU I, *et al.* J Phys G, 2005, **31**: 1303.
[5] XU F R, WALKER P M, WYSS R. Phys Rev C, 2002, **65**: 021303(R).
[6] NAZAREWICZ W, DOBACZEWSKI J, MATEV M, *et al.* Acta Phys Pol B, 2001, **32**: 2349.
[7] ZHU S J, HAMILTON J H, RAMAYYA A V, *et al.* Eur Phys J A, 2005, 25 Supl. **1**: 459.
[8] ZHANG X Q, HAMILTON J H, RAMAYYA A V, *et al.* Phys Rev C, 2001, **63**: 027302.
[9] LUO Y X, WU S C, GILAT J, *et al.* Phys Rev C, 2004, **69**: 024315.
[10] LUO Y X, HAMILTON J H, RASMUSSEN J O, *et al.* Phys Rev C, 2006, **74**: 024308.
[11] WANG Y, RINTA ANTILA S, DENDOOVER P, *et al.* Phys Rev C, 2003, **67**: 064303.
[12] OHYA S, MUTSURO N, MATUMOTO Z, *et al.* Nucl Phys A, 1980, **334**: 382.
[13] BOHR A, MOTTELSON B R. Nuclear structure, Benjamin[M]. New York: 1975: 2.
[14] YANG F, HAMILTON J H. Modern Atomic and Nuclear Physics[M]. Singapore: World Scientific, 2010.
[15] HAMILTON J H, RAMAYYA A V, PINKSTON W T, *et al.* Phys Rev Lett, 1974, **32**: 239.
[16] PIERCEY R B, HAMILTON J H, SOUNDRANAYAGAM R, *et al.* Phys Rev Lett, 1981, **47**: 1514.
[17] MÖLLER P, BENGTSSON R, CARLSSON B G, *et al.* Phys Rev Lett, 2006, **97**: 162502.
[18] KOICHI S, NOBUO H. Nucl Phys A, 2011, **849**: 53.
[19] TAJIMA N, SUZUKI N. Phys Rev C, 2011, **64**: 037301.
[20] FISCHER S M, BALAMUTH D P, HAUSLADEN P A, *et al.* Phys Rev Lett, 2000, **84**: 4064.
[21] MÖLLER P, NIX J R, MYERS W D, *et al.* At Data Nucl Data Tables, 1995, **59**: 185.
[22] ÄYSTÖJ, JAUHO P P, JANAS Z, *et al.* Nucl Phys A, 1990, **515**: 365.
[23] FRAUENDORF S, MENG J. Nucl Phys A, 1997, **617**: 131.
[24] LUO Y X, ZHU S J, HAMILTON J H, *et al.* Phys Lett B, 2009, **670**: 307.
[25] TIMAR J, VAMAN C, STAROSTA K, *et al.* Phys Rev C, 2006, **73**: 011301(R).
[26] LU Q H, BUTLEr-MOORE K, ZHU S J, *et al.* Phys Rev C, 1995, **52**: 1348.
[27] SHANNON J A, PHILLIPS W R, DURELL J L, *et al.* Phys Lett B, 1994, **336**: 136.
[28] HAMILTON J H, RAMAYYA A V, HWANG J K, *et al.* Eur Phys J A, 2002, **15**: 175.
[29] SMITH A G, DURELL J L, PHILLIPS WR, *et al.* Phys Rev Lett, 1996, **77**: 1711.
[30] LUO Y X, RASMUSSEN J O, HAMILTON J H, *et al.* Nucl Phys A, 2013, **919**: 67.
[31] HAMILTON J H, ZHU S J, LUO Y X, *et al.* Nucl Phys A, 2010, **834**: 28c.
[32] FRAUENDORF S, *et al.*, to be published.
[33] CAPRIO M, Phys Rev C, 2011, **83**: 064309.
[34] HWANG J K, RAMAYYA AV, HAMILTON J H, *et al.* Phys Rev C, 2002, **65**: 054314.

[35] TIMAR J, KOIKE T, PIETRALLA N, *et al*. Phys Rev C, 2007, **76**: 024307.
[36] WANG Z G, LIU M L, ZHANG Y H, *et al*. Phys Rev C, 2013, **88**: 024306.
[37] HE C Y, ZHU L H, WU X G, *et al*. Phys Rev C, 2010, **81**: 057301.
[38] YAO S H, MA H L, ZHU L H, *et al*. Phys Rev C, 2014, **89**: 014327.
[39] SETHI J, PALIT R, SAHA S, *et al*. Phys Lett B, 2013, **725**: 85.
[40] DATTA P, ROY S, PAL S, *et al*. Phys Rev C, 2008, **78**: 021306(R).
[41] ROY S, RATHER N, DATTA P, *et al*. Phys Lett B, 2012, **710**: 587.
[42] GARRETT P F, WOOD J L, J Phys G, 2010, **37**: 064028.
[43] LUO Y X, RASMUSSEN J O, NELSON C S, *et al*. Nucl Phys A, 2012, **874**: 32.
[44] FRAUENDORF S, GU Y, SUN J, *et al*. Inter Jour of Modern Phys E, 2011, **20**: 465.
[45] CHAMOLI S K, STRUCHBERY A E, FRAUENDORF S, *et al*. Phys Rev C, 2011, **83**: 054318.
[46] ILIEVA S, THŰRAUF M, KRÖLL TH, *et al*. Phys Rev C, 2014, **89**: 014313.
[47] HUA H, WU C Y, CLINE D, *et al*. Phys Rev C, 2004, **69**: 014317.
[48] NAVIN A, REJMUND M, SCHMITD C, *et al*. Phys Lett B, 2014, **728**: 136.
[49] GUESSOUS A, SCHULZ N, PHILLIPS W R, *et al*. Phys Rev Lett, 1995, **75**: 2280.
[50] GUESSOUS A, SCHULZ N, BENTALEB M, *et al*. Phys Rev C, 1996, **53**: 1191.
[51] DING H B, ZHU S J, HAMILTON J H, *et al*. Phys Rev C, 2006, **74**: 054301.
[52] URBAN W, RZACA-URBAN T, DURELL J L, *et al*. Eur Phys J A, 2004, **20**: 381.
[53] JONES E F, GORE P M, ZHU S J, *et al*. Phys Atomic Nucl, 2006, **69**(7): 1198.
[54] LUO Y X, HAMILTON J H, RASMUSSEN J O, *et al*. Chin Nucl Phys Rev, 2010, **27**(3): 229.
[55] HWANG J K, RAMAYYA A V, GILAT J, *et al*. Phys Rev C, 1998, **58**: 3252.
[56] HWANG J K, RAMAYYA A V, HAMILTON J H, *et al*. J Phys G: Nucl Part Phys, 2001, **27**: L9.
[57] WANG J G, ZHU S J, HAMILTON J H, *et al*. Phys Rev C, 2008, **78**: 014313.
[58] LUO Y X, RASMUSSEN J O, HAMILTON J H, *et al*. Nucl Phys A, 2009, **825**: 1.
[59] LUO Y X, RASMUSSEN J O, HAMILTON J H, *et al*. Phys, Rev C, 2014, **89**: 044326.
[60] WANG J G, ZHU S J, HAMILTON J H, *et al*. Phys Lett B, 2009, **675**: 420.
[61] LI H J, ZHU S J, HAMILTON J H, *et al*. Phys Rev C, 2013, **88**: 054311.
[62] HAMILTON J H, RAMAYYA A V, ZHU S J, *et al*. Prog Part Nucl Phys, 1995, **35**: 635.
[63] BAXTER A M, KHOO T L, BLEICH M E, *et al*. Nucl Instrum Methods A, 1992, **317**: 101.
[64] RADFORD D C, Nucl Instr Meth A, 1995, **317**: 297; also cf. his website http://radware.phy.ornl.gov/
[65] DANIEL A, GOODIN C, LI K, *et al*. Nucl Instrum Methods B, 2007, **262**: 399.
[66] HAUSTEIN P E, TAYLOR H W, MCPHERSON R, *et al*. Nucl Data Tables A, 1972, **10**(4/5): 321.
[67] TAYLOR H W, SINGH B, PRATO F S, *et al*. Nucl Data Tables A, 1971, **9**: 1.
[68] JOSHI P, CARPENTER M P, FOSSAN D B, *et al*. Phys Rev Lett, 2007, **98**: 102501.
[69] HOURY M, LUCAS R, PORQUET M G, *et al*. Eur Phys J A, 1999, **6**: 43.
[70] ZHANG X Q, HAMILTON J H, RAMAYYA AV, *et al*. Phys Rev C, 2000, **61**: 014305.
[71] KRÜCKEN R, ASZTALOS S J, CLARK R M, *et al*. Eur Phys J A, 2001, **10**: 151.
[72] STOYER M A, WALTERS W B, WU C Y, *et al*. Nucl Phys A, 2007, **787**: 455c.
[73] URBAN W, ZLOMANIEC A, SIMPSON G, *et al*. Eur Phys J A, 2004, **22**: 157.
[74] HARTLEY D J, JANSSENS R V F, RIEDINGER L L, *et al*. Phys Rev C, 2009, **80**: 041304(R).
[75] YEOH E Y, ZHU S J, HAMITON J H, *et al*. Phys Rev C, 2011, **83**: 054317.
[76] STEFANESCU I, GELBERG A, JOLIE J, *et al*. Nucl Phys A, 2007, **789**: 125.
[77] DELAROCH J.-P, GIROD M, LIBERT J, *et al*. Phys Rev C, 2010, **81**: 014303.
[78] JOSHI P, WILKINSEN A R, KOIKE T, *et al*. Eur Phys J A, 2005, **24**: 23.
[79] LIU Y X. *et al*. to be published.

# 质子数 Z 分别位于 Ru 之上和之下的 $A\sim(100\sim126)$ 丰中子原子核三轴形变在原子核形状变迁和共存中的重要作用

Y. X. LUO (罗亦孝)[1, 2, 1)], J. H. Hamilton[1], J. O. Rasmussen[2, 3], A.V. Ramayya[1], S. Frauendorf[4, 5], E. WANG (王恩宏)[1], J. K. Hwang[1], J. G. WANG (王建国)[6], H. J. LI (李红洁)[6], E. Y. Yeoh (杨韵颐)[6], S.J. ZHU (朱胜江)[1, 6], Y. X. LIU (刘艳鑫)[7], C. F. JIAO (焦长峰)[8], W. Y. LIANG (梁午阳)[8], Yue SHI (石跃)[8], F. R. XU (许甫荣)[8], Y. SUN (孙扬)[9, 10], S. H. LIU (刘少华)[1, 11], N. T. Brewer[1, 12], I. Y. Lee[2], G.M. Ter-Akopian[13], A. V. Daniel[13], Yu. Oganessian[13], M. A. Stoyer[14], R. Donangelo[15], W. C. MA (马文超)[16]

(1. Physics Department, Vanderbilt University, Nashville, TN 37235, USA;
2. Lawrence Berkeley National Laboratory, Berkeley, CA 94720, USA;
3. Department of Chemistry, U.C. Berkeley, Berkeley, CA 94720, USA;
4. Department of Physics, University of Notre Dame, Notre Dame IN 46556, USA;
5. Institut für Strahlenphysik, FZD-Rossendorf, Postfach, D-01314 Dresden, Germany;
6. Department of Physics, Tsinghua University, Beijing 100084, China;
7. School of Science, Huzhou Teachers College, Huzhou 31300, Zhejiang, China;
8. School of Physics, Peking University, Beijing 100871, China;
9. Department of Physics and Astronomy, Shanghai Jiao Tong University, Shanghai 200240, China;
10. Institute of Modern Physics, Chinese Academy of Sciences, Lanzhou 730000, China;
11. Chemistry Department, University of Kentucky, Lexington, KY 40505, USA;
12. Physics Division, Oak Ridge National Laboratory, Oak Ridge, TN 37831, USA;
13. Flerov Laboratory for Nuclear Reactions, JINR, Dubna 141980, Russia;
14. Lawrence Livermore National Laboratory, Livermore, CA 94550, USA;
15. Instituto de Fisica, Facultad de Ingenieria, C.C. 30, 11300 Montevideo, Uruguay;
16. Physics Department, Mississippi State University, Mississippi State, MS 39762, USA )

**摘要：** 基于Ru ($Z=44$) 丰中子同位素中存在最大三轴形变的理论预言和实验证据，综述了近年来Rh ($Z=45$), Pd ($Z=46$), Ag ($Z=47$), Cd ($Z=48$)(质子数 $Z$ 位于Ru，$Z=44$之上)及Zr ($Z=40$), Nb ($Z=41$), Mo ($Z=42$), Tc ($Z=43$)(质子数 $Z$ 位于Ru，$Z=44$之下) 的 $A\sim(100\sim126)$ 丰中子同位素中关于三轴形变的形状变迁和形状共存系统性研究的重要进展。$^{252}$Cf 自发裂变瞬发 γ 射线 γ-γ-γ 三重符合、特别是新建立的 γ-γ-γ-γ 四重符合数据的系统观测和研究，在Ru, Pd, Cd和Nb 丰中子同位素中显著扩展或首次观测到了一系列能带，为这个核区原子核形状的研究提供了新的、重要的实验数据。联系此前报道的有关进展，使用PES, TRS, PSM, CCCSM和SCTAC理论模型计算拟合新的实验数据，在该核区沿同中素和同位素链，并随自旋和激发能变化各自由度，跟踪原子核形状渐进变化，获得了新的系统性研究成果，显著扩展和深化了人们对原子核形状变迁和形状共存的认知。

对于Ru及其上的Rh ($Z=45$), Pd ($Z=46$), Ag ($Z=47$) 和Cd ($Z=48$) 丰中子同位素的研究表明：Rh 丰中子核具有比最大值稍小的三轴形变，$\gamma=-28°$，并在 $^{103-106}$Rh 同位素链上鉴别出了手征对称破缺；在三轴形变核$^{112}$Ru和$^{114}$Pd($N=68$)中发现了三轴原子核的摆动运动，该摆动运动也可能在$^{114}$Ru ($N=70$)中存在；观察到了从具有最大三轴形变的$^{110,112}$Ru 中手征破缺到稍小三轴形变的$^{112,114,116}$Pd 中扰动的手征破缺的过渡；在较软的Ag 核中观察到了丰富的谱学结构，在$^{104,105}$Ag 中鉴别出了可能的手征对称破缺，在较重的$^{115,117}$Ag 中提出了

**收稿日期：** 2014-09-01； **修改日期：** 2014-11-24

**基金项目：** 美国能源部基金资助项目(DE-FG-05-88ER40407, DE-AC02-05CH11231, DE-FG02-95ER40934, DE-AC05-00OR22725, DE-AC52-07NA27344, DE-FG02-95ER40939)；国家自然科学基金资助项目(11175095, 10975082, 11235001, 11320101004, 11305059, 11275063, 11275068, 11135005, 11075103)；教育部重点基金项目(2010000211007)；国家重点基础研究计划项目(973计划)(2013CB834401)；俄罗斯基础研究基金会项目(11-02-12050, 11-02-12066)

1) E-mail: yxluo@lbl.gov。

趋于三轴形变的$\gamma$软度；具有小形变的Cd核的能级结构被解释为准粒子耦合、准转动和软三轴形变；最近的库伦激发的研究提供了$Z=50$, $N=82$满壳附近$^{122,124,126}$Cd 核中出现核集体性的实验和理论证据；上述研究成果展现出从Ru中的最大三轴形变($\gamma=-30°$，三轴形变极小增益为0.67 MeV), 经具有大三轴形变的Rh核($\gamma=-28°$)，到Pd核中的稍小、但稳定于中等自旋到高自旋区的三轴形变($\gamma\sim-41°$，三轴形变极小增益为0.32 MeV)，再经Ag核中的$\gamma$软度，最后到具有很小形变、但仍出现集体性质、包括软三轴形变的Cd核的过渡。对于Pd核转动带交叉系统性的研究揭示了其第一带交叉$(\nu h_{11/2})^2$ 中子转动顺排的上行$\gamma$驱动，和第二带交叉$(\pi g_{9/2})^2$质子转动顺排的下行$\gamma$驱动效应，成功地解释了$^{114}$Pd 中的三轴摆动运动，并给出了$^{110\text{-}118}$Pd同位素链中理论早已预言、而比早期理论预言更为完整准确的形状渐进变迁和形状共存的图像。根据该核区的系统研究，发现最大三轴形变出现在$^{112}$Ru，而在相邻的偶$Z$(Pd)同位素链，三轴形变极小的中心在$^{114}$Pd, 两者均为$N=68$。上述系统性研究沿相邻的Ru和Pd偶$Z$同位素链，在$N=68$同中素中鉴别出最大三轴形变，均比理论预言的$^{108}$Ru 和$^{110}$Pd 多4个中子。

在$Z$值位于Ru ($Z=44$) 之下的Zr ($Z=40$), Nb ($Z=41$), Mo ($Z=42$) and Tc ($Z=43$) 丰中子同位素中，Y和Zr核具有很强的轴对称四极形变，而在较重的Zr同位素中出现了$\gamma$自由度；较重的Nb核($A=104\sim106$) 基态具有中等程度的软三轴形变和强四极形变，随着自旋和激发能的增加，过渡到接近于轴对称的强四极形变；而较轻的Nb核($A\leqslant103$) 基态均接近轴对称形状；在Nb同位素链上基态由球形到强四极形变的形状突变发生在$^{100}$Nb ($N=59$)，在$^{100\text{–}106}$Nb同位素链中基态的软三轴形变随中子数增加而增加；在Nb核中还观察到关于软三轴形变的形状共存；Mo核具有大的三轴形变，观察到了$\gamma$振动和手征对称破缺；Tc核具有比最大值稍小的三轴形变，$\gamma=-26°$，并观察到了手征对称破缺。

质子数$Z$从41到48的$A\sim(100\sim126)$丰中子同位素，特别是Pd和Nb 同位素，呈现出关于三轴形变的过渡特征。

**关键词：** 质子数从41到48范围的丰中子核；原子核形状变迁和共存；长椭球到扁椭球形状变迁；三轴形变；三轴形变原子核摆动运动；原子核手征对称破缺；扰动手征态；$\gamma$振动能带；高自旋态；带交叉；$\gamma$驱动效应；准转动；$Z=50$和$N=82$闭壳附近集体性和软三轴形变的出现；能级纲图；原子核能级自旋/宇称/组态指定；位能面(PES)；投影壳模型(PSM)；总Routhian面(TRS)；推转和组态限制壳模型(CCCSM) 和壳修正斜轴推转模型(SCTAC) 理论计算；自发裂变瞬发$\gamma$谱学；$\gamma$射线三重和四重符合及角关联测量；锎−252；Gammasphere 多探测器系统